MISSION ORIENTED ADVANCED NUCLEAR SYSTEM PARAMETERS STUDY

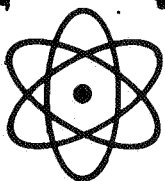MARCH 1965

FINAL REPORT

DRA

VOLUME I

8423-6005-RU000

SUMMARY TECHNICAL REPORT

FOR

GEORGE C. MARSHALL SPACE FLIGHT CENTER

BY

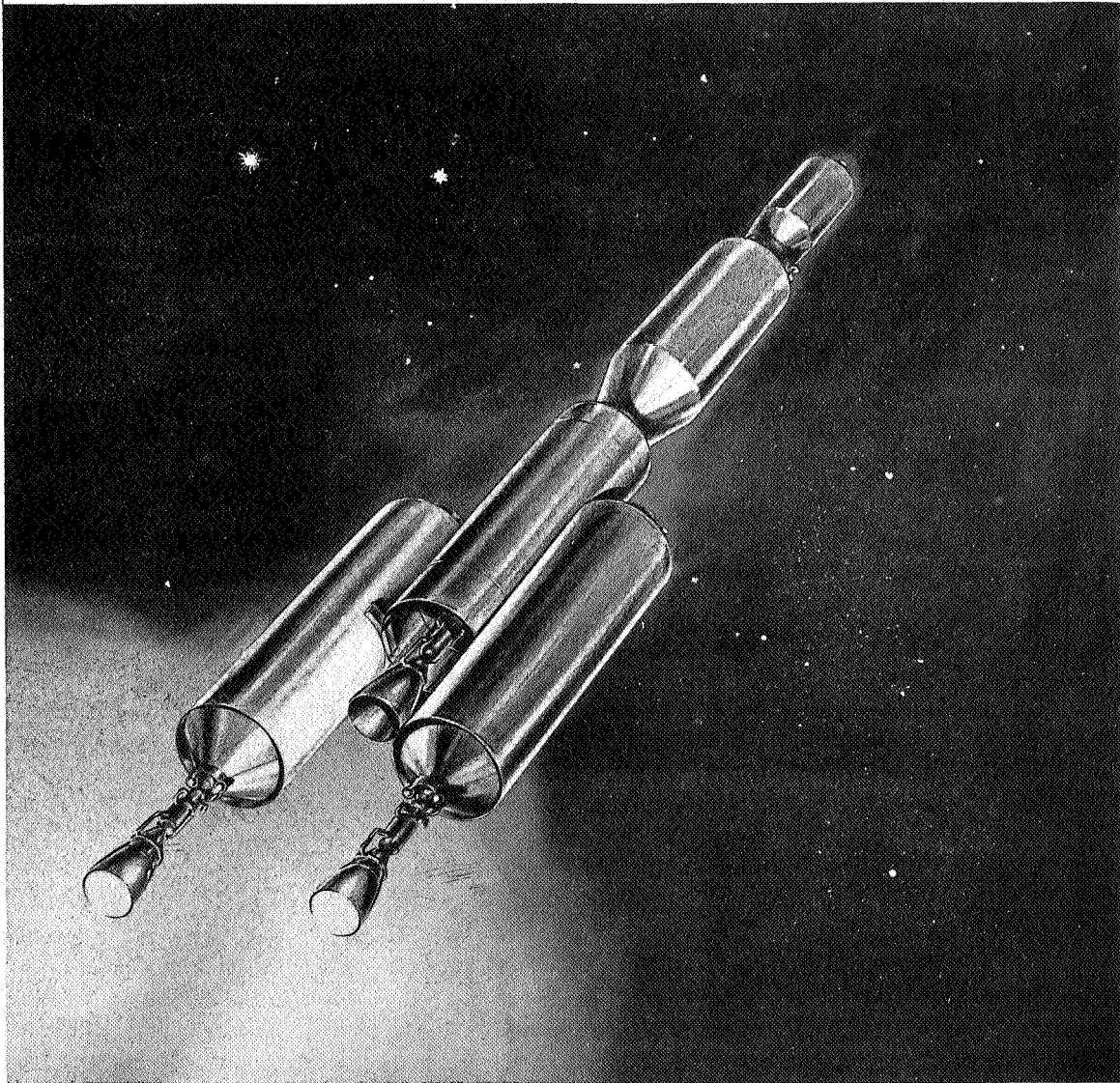***TRW*** *SPACE TECHNOLOGY LABORATORIES*

THOMPSON RAMO WOOLDRIDGE INC.

MISSION ORIENTED ADVANCED NUCLEAR SYSTEM

PARAMETERS STUDY

Final Report
Volume I

Summary Technical Report

for

George C. Marshall Space Flight Center
National Aeronautics and Space Administration

by
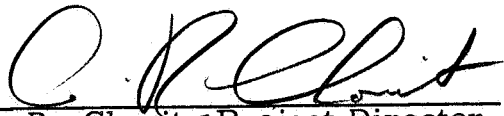
TRW Space Technology Laboratories
Redondo Beach, California

Volume I   Summary Technical Report

Prepared By: A. R. Chovit, Systems Research and Engineering Laboratory

Dr. R. K. Plebuch, Nuclear Technology Department

Dr. C. D. Kylstra, Nuclear Technology Department

Approved:

A. R. Chovit, Project Director
Mission Oriented Advanced Nuclear
System Parameter Study

Dr. D. Jortner, Manager
Nuclear Technology Department

Dr. P. Dergarabedian, Director
Systems Research and Engineering Laboratory

FOREWORD

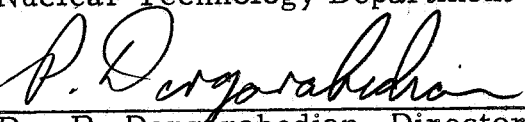This volume, which is one of a set of nine volumes, describes in part the studies, analyses, and results that were accomplished under contract NAS8-5371, Mission Oriented Advanced Nuclear Systems Parameters Study, for George C. Marshall Space Flight Center, Huntsville, Alabama. This work was performed during the period from April 1963 to March 1965 and covers Phases I, II, and III of the subject contract.

This final report has been organized into nine separate volumes on the basis of contractual requirements and to provide a useful and manageable set of documents. The volumes in this set are:

Volume I	Summary Technical Report
Volume II	Detailed Technical Report; Mission and Vehicle Analysis
Volume III	Parametric Mission Performance Data
Volume IV	Detailed Technical Report; Nuclear Rocket Engine Analysis
Volume V	Nuclear Rocket Engine Analysis Results
Volume VI	Research and Technology Implications Report
Volume VII	Computer Program Documentation; Mission Optimization Program; Planetary Stopover and Swingby Missions
Volume VIII	Computer Program Documentation; Mission Optimization Program; Planetary Flyby Mission
Volume IX	Computer Program Documentation; Nuclear Rocket Engine Optimization Program

Volumes I, II, and IV include the details of the study approach and basic guidelines, the analytic techniques developed, the analyses performed, the results obtained and an evaluation of these results together with specific conclusions and recommendations. Volumes III and V contain parametric mission, vehicle, and engine data and results primarily in graphical form. These data present the interrelationships existing among the parameters that define the mission, vehicle, and engine. Volume VI delineates those areas of research and technology wherein further efforts would be desirable based on the results of the study. Volumes VII through IX describe the computer programs developed and utilized during the study and present instructions and test cases to enable operation of the programs.

ABSTRACT

A summary of the study approach, basic guidelines, and assumptions that were used in a comprehensive, parametric lunar and interplanetary mission and solid core, nuclear engine analysis are given. The analyses performed and the analytic techniques generated in developing three analysis computer programs for the IBM 7094 are summarized. These three programs, the SWingby Optimization Program (SWOP), the FLyby Optimization Program (FLOP), and the Nuclear Rocket Engine Optimization Program (NOP) were employed to generate over 20,000 mission simulations, and to investigate the effect on engine and vehicle performance of variations in nuclear engine design parameters and constraints. A summary of the results is presented which establishes an optimum thrust range for the advanced nuclear engine, determines the design characteristics of a compromise advanced nuclear engine, and establishes the sensitivity of the vehicle to variations in mission, engine, and vehicle parameters and modes.

CONTENTS

ILLUSTRATIONS

ILLUSTRATIONS

TABLES

I INTRODUCTION

This final report summarizes the mission, vehicle, and engine analyses and the results of Phases I, II, and III of the Mission Oriented Advanced Nuclear System Parameters Study performed by TRW Space Technology Laboratories for the George C. Marshall Space Flight Center.

STUDY OBJECTIVE

The basic overall objectives of this study consisted of the following:

o   Derivation and computer programming of analytical models for evaluating the various nuclear engine, vehicle system, and mission parameters for nuclear propulsion system applications in the 1975 - 1990 time period.

o   Produce the necessary propulsion and system parametric data and criteria based on probable missions to permit NASA to identify and define the essential design requirements for an operational nuclear propulsion system or systems for the 1975 - 1990 time period.

o   Recommend to NASA preliminary design characteristics of the nuclear propulsion system which results in the best compromise for lunar, planetary flyby, and planetary stopover missions.

STUDY APPROACH

It is evident that no simple criteria are readily available upon which the selection of the "optimum" engine may be based. The engine, or engines, should be a compromise for a large majority of possible missions in the chosen time period. The performance of the engine should be biased toward the performance requirements of the missions of greatest importance and the missions requiring the largest number of flights. Furthermore, the selected nuclear engines must meet the requirements of demonstrated technical feasibility and be capable of development by the time of operational application. In this assessment, it is necessary to review the state-of-the-art concerning materials and component technology in order to arrive at rational predictions of future development capability. Finally, the vehicle which utilizes the compromise engine must be compatible with the launch and payload constraints of the boost vehicles for this time period.

In order to analyze and evaluate the mission utility of a nuclear propulsion system, it was necessary to formulate a study approach that would reflect all of the complex interactions between the engine, mission, and vehicle parameters. Furthermore, parametric relationships had to be established with sufficient accuracy such that the results of the study would not be invalidated. The goal in this study was to develop, for the first time, efficient methods of carrying out parametric analyses which preserve the accuracy inherent in detailed calculations of individual subsystems.

Figure I-1 shows a graphical representation of the approach adopted for the overall study. The key elements in this approach are listed at the bottom of the chart.

PARTING
PLANE

```
┌─────────────┐         ┌─────────────┐              ┌─────────────┐
│ PROPULSION  │         │CONFIGURATION│              │ MISSION AND │
│ AND ENGINE  │────────▶│ AND DESIGN  │              │ TRAJECTORY  │
│  ANALYSIS   │         │  ANALYSIS   │              │  ANALYSIS   │
└─────────────┘         └─────────────┘              └─────────────┘

                        ┌─────────────┐              ┌─────────────┐
                        │             │              │ PARAMETRIC  │
                        │  WEIGHTS    │              │ PERFORMANCE │
                        │  ANALYSIS   │              │ EVALUATION  │
                        └─────────────┘              └─────────────┘

                                                     ┌─────────────┐
                                                     │ PERFORMANCE │
                                                     │ EVALUATION  │
                                                     │   OUTPUT    │
                                                     └─────────────┘
```

STAGED ANALYSIS
INTEGRAL VERSUS DIFFERENTIAL CALCULATIONS
PARTING PLAN PARAMETERS
OUTPUT INTERPRETATION
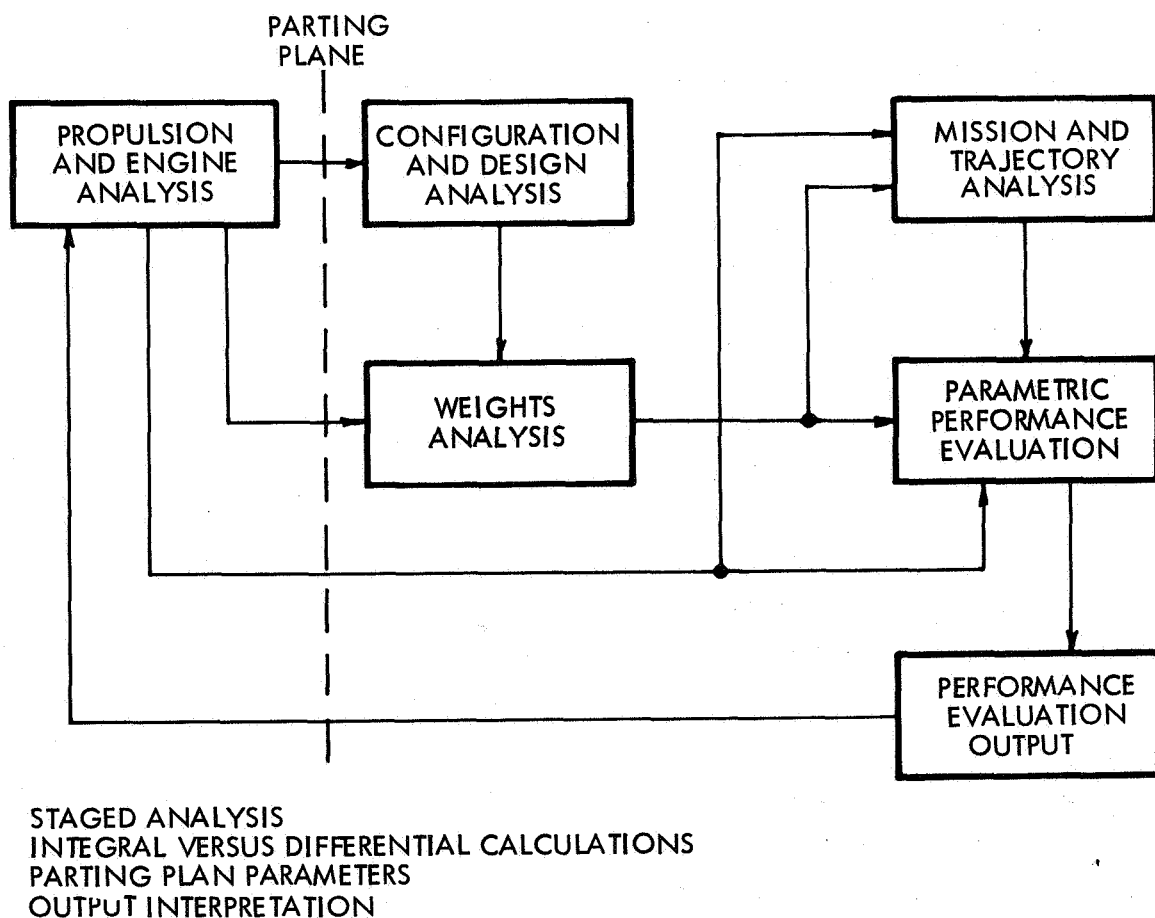
Figure I-1 Study Approach

First and foremost is the concept of "Staged Analysis". This concept refers to the separation of major subsystem parametric analyses into individual segments or stages for each major subsystem. In this way, each individual subsystem could be analyzed independently in order to derive the integral scaling laws so essential for the efficient parametric analysis of complex systems. The development of reliable integral scaling laws from detailed differential calculations allowed the treatment of each subsystem in a "black box" fashion, characterizing each subsystem solely by its principal input and output variables.

Figure I-1 shows each of these principal logic areas as boxes in a functional flow chain of information. However, the box concerning the nuclear propulsion system is separated from the remainder of the logic and information content by a "Parting Plane". All exchange of information between the engine analysis and system performance areas of effort must occur through this parting plane. Engine performance at the parting plane is characterized by three basic performance parameters; engine specific impulse, engine thrust, and engine weight. These three variables provide the principal links between the engine and the vehicle. The single parting plane parameter characterizing the vehicle performance is the total vehicle weight in Earth orbit required to deliver a given payload weight for the mission specified. The study approach outlined can be used to determine the sensitivity and interactions among the engine, vehicle, and mission parameters.

Figure I-2 is a functional diagram showing the interrelationships of the major task categories, task inputs and outputs, and computer programs. It is analogous on a functional level to the previous figure indicating the study approach.

The rectangular boxes represent the computer programs that were developed in the course of the study. The Nuclear Rocket Engine Optimization Program (NOP) produces the optimum reactor and engine performance parameter relationships while the mission analysis programs, the FLyby Optimization Program (FLOP) and SWingby Optimization Program (SWOP), determine the required minimum vehicle weight for any given set of engine performance parameters, vehicle configurations, or mission constraints. The hexagonal boxes represent the analyses performed in order to generate the required inputs from the configuration design, trajectory, and weight studies.

I-3
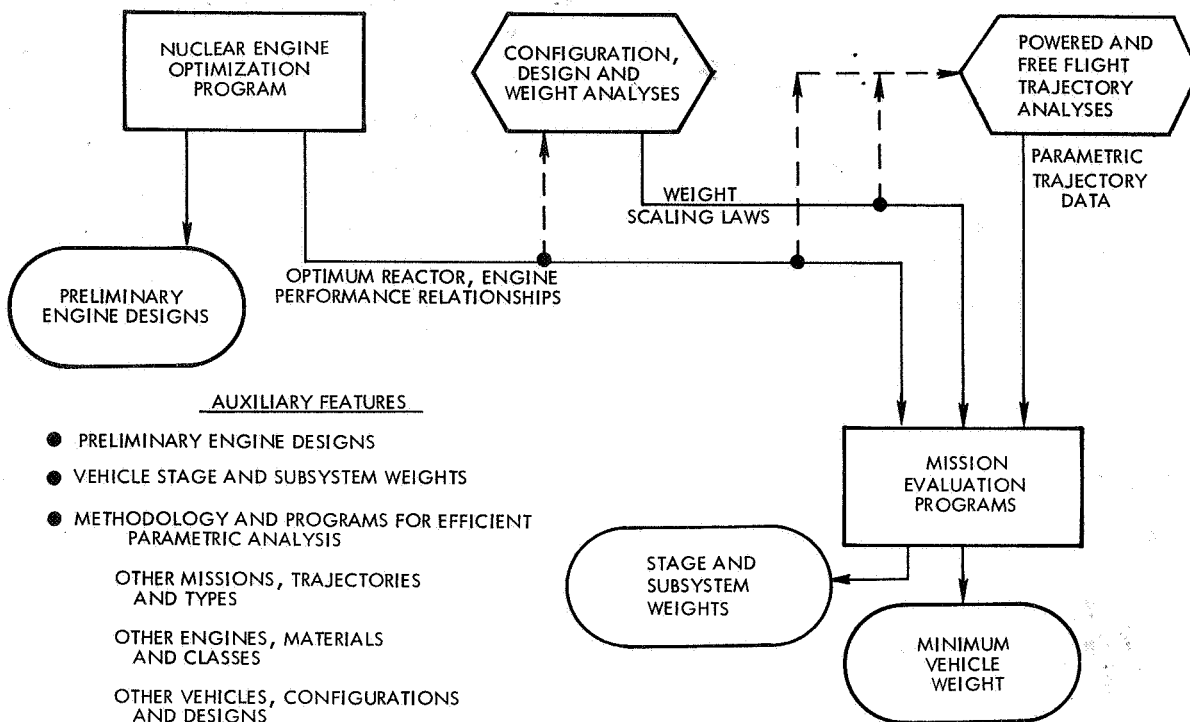
Figure I-2 Performance Evaluation of Nuclear Systems

The nuclear engine and mission analysis computer programs inherently produce outputs of considerable value quite apart from the basic objectives of the overall study. Not only do the programs give optimum nuclear engine and minimum vehicle weight information, but each yields preliminary weights, sizes, and designs for given sets of flight or operating specifications. In the operation of these programs, these outputs can be made optimum or non-optimum as desired. The considerable complexity of accurate determination of optimum interplanetary flight trajectories for any given set of engine performance and vehicle configuration criteria required the utilization of a new and unique method of analysis. The methods developed constitute a major advance in the methodology of mission and trajectory analysis. Similarly the overall design of nuclear rocket engines is an extremely complicated undertaking, compounded by numerous design constraints placed on the engine. The conception and construction of the Nuclear Rocket Engine Optimization Program marked a major step forward in improving the accuracy of parametric nuclear engine analysis and design capability by utilizing differentially calculated results.

The basic methodology, concepts, and computer programs developed during the study already have found application to a wide variety of other mission analyses of interest in the investigation of interplanetary space travel. The versatility and adaptability of the programs permitted, during the course of the study, the expansion of the scope of work to include non-nuclear propulsion configurations, powered and unpowered swingby trajectories, variable tank scaling laws, trip time constraints, upgrading existing engine designs, and the evaluation of different nuclear engine designs.

STUDY PLAN

The overall study was divided into three study phases, the first of which was the "identification" phase. During this phase, the principal objectives were 1) to develop an efficient and accurate methodology for the rapid analysis and comparison of advanced nuclear engine systems, 2) to establish the necessary constraints and guidelines to allow the successful application of this methodology in the second phase of this study, and 3) to evaluate the scope and level of effort appropriate to the second phase of work.

The second phase of the study was concerned with developing the computer programs which would be used to analyze the engine design parameters in terms of the engine thrust, specific impulse, and weight and then determining the influence of engine performance on the required vehicle weight. The development of these computer programs required detailed analyses of interplanetary trajectories, nuclear engines, and the spacecraft in order to determine the required scaling laws, data, and correlations which would relate the pertinent variables for each major subsystem of the complete engine and vehicle. The scaling laws and correlations were then coupled by appropriate calculational techniques and functional equations to provide the parametric description of the integrated mission/vehicle/engine system. Digital computer programs were developed in order to perform the large number of computations necessary for the parametric analyses required by the scope of this study.

In the third phase of the study, these computer programs were utilized to obtain the relationships existing among the parameters that define the mission, the vehicle configuration, the nuclear propulsion system, and the performance of the overall vehicle for interplanetary and lunar missions. These relationships clearly indicated the relative importance and sensitivity of the nuclear engine design parameters on the overall vehicle performance for the range of engine, vehicle, and mission parameters established in Phase I. The results obtained from the computer runs also showed the influence of 1) the various modes of engine usage, e. g. , clustered vs single engines, or nuclear engine aftercooling, 2) vehicle design and operation, e. g. , propellant tank mass fractions, payload weight, or non-nuclear (chemical) propulsion stages, and 3) trajectory perturbations, e. g. , planet destinations, trip times, or mission years.

The mission evaluation programs were utilized to analyze the parting plane parameters to determine the best compromise engine thrust level for interplanetary missions in the 1975 to 1990 time period. Primarily, the initial vehicle weight and maximum engine firing time were determined as a function of thrust level and various mission modes and mission years. Following the determination of this compromise thrust, a detailed analysis was made to determine the vehicle and stage weight sensitivity to variatio ns in performance, vehicle, and mission parameters. These variations included payload weights, stage mass fractions, engine weights, thrust, specific impulse, propellant types, aerodynamic braking, propellant boil-off, stopover time, and mission year. Concurrently, the nuclear engine optimization computer program was used for analyzing the detailed engine design para-meters in terms of their effect on the parting plane parameters, i. e. , the engine weight, thrust, and specific impulse.

In this manner, it was possible to determine within a narrow range the mission, vehicle, and engine performance requirements for future manned interplanetary missions. Within this narrow range, a more detailed analysis was then performed which related the vehicle and mission requirements to variations in specific engine design parameters. These parametric results permitted the determination and evaluation of the requirements for the design and development of the various optimum vehicle and engine configurations. This portion of the study provided an assessment of the criteria for the successful development of optimum engine and vehicle combinations and determined the influence of various major or critical state-of-the-art advancements on engine and vehicle performance. Similarly, a definition and evaluation of vehicle design problems, requirements, criteria, and constraints were made as influenced by the range of nuclear engine design parameters.

The information obtained from these detailed assessments then permitted the identification of the design requirements for the engine of maximum utility together with major vehicle and mission criteria. A preliminary engine and vehicle design was then performed for the recommended engine and vehicle. The final result of this study is a detailed set of engine specifications which outline the basic engine and reactor performance and design requirements for the selected compromise nuclear propulsion system (Volumes IV and V). Additional specifications include a set of constraints and requirements for the remaining portions of the vehicle system for each specific mission of major interest (Volumes II and III). The combined set of engine and vehicle specifications in turn define the performance characteristics which can be expected from vehicles propelled by the selected nuclear engine for interplanetary flight missions in the 1975 to 1990 time period.

II STUDY ASSUMPTIONS, CONSTRAINTS, AND SCALING LAWS

Initially, a set of assumptions and constraints were postulated for the study in order to circumscribe certain mission types and modes, the engine designs, the vehicle configurations, the mission operational criteria, and the scope of analyses and computational procedures.

MISSION

Mission Types

The basic set of missions to be investigated consisted of the following:

- o   Manned Mars stopover mission
- o   Manned Venus stopover mission
- o   Manned Mars flyby mission
- o   Manned Venus flyby mission
- o   Manned Mars/Venus swingby mission
- o   Lunar transfer mission

Stopover Mission

A typical stopover mission is shown on Figure II-1, which depicts the major operational phases and vehicle weight changes that occur during the mission. Additional vehicle weight requirements are included for life support expendables, propellant boil off, and attitude control. If an aerodynamic braking mode is employed at the target planet, a propulsive velocity change is used for circularizing or adjusting the resulting orbit. The Earth braking propulsive retro can be eliminated by option and an all aerodynamic Earth braking mode employed. All opposition years from 1975 to 1990 were to be considered for the Mars mission; 1980 for the Venus mission.

Stopover Mission Trajectory Type

Two types of trajectories were considered for the stopover missions, designated type IB and type IIB. The "B" denotes an inbound trajectory leg where the heliocentric angle traversed, θ, is greater than 180° and less than 360°; the "I" denotes an outbound trajectory leg where $180^{\circ} < \theta < 360^{\circ}$; the "II" designates an outbound trajectory leg where $0^{\circ} < \theta < 180^{\circ}$. The total trip time for a type IB mission is characteristically between 500 and 550 days; for type IIB between 400 and 450 days.

STAGE I FIRED

OUTBOUND MIDCOURSE
CORRECTIONS

OUTBOUND MIDCOURSE
STAGE JETTISONED

STAGE II FIRED

STAGE I JETTISONED

MEM LANDS ON MARS

MEM LEAVES MARS

MEM DOCKS WITH
MISSION MODULE

STAGE II JETTISONED

MEM EJECTED

STAGE III JETTISONED

MISSION MODULE AND
INBOUND MIDCOURSE STAGE
STAGE JETTISONED

MEM PROPULSION
STAGE JETTISONED

STAGE III FIRED

INBOUND MIDCOURSE
CORRECTIONS

STAGE I —— LEAVE EARTH
STAGE II —— MARS BRAKING
STAGE III —— LEAVE MARS
MEM —— MARS ENTRY MODULE

EARTH RETRO FIRED

EARTH RETRO STAGE
JETTISONED

CAPSULE RETURNS TO
EARTH AFTER
AERODYNAMIC BRAKING

Figure II-1 Mars Stopover Mission Sequence

Swingby Mission

A swingby mission is essentially the same as a Mars stopover mission except the trajectory is constrained to pass in the vicinity of the planet Venus either during the outbound or inbound leg. The vehicle, therefore, performs a hyperbolic turn about Venus. For the swingby mission, a third midcourse correction propulsion maneuver is assumed.

Flyby Mission

Characteristically, the operational sequence for the flyby mission is identical to that of the stopover mission except the vehicle does not go into orbit about Mars. Thus, the two velocity changes at the target planet are eliminated, i. e. , the arrive planet braking and leave planet boost phases. Low energy trajectories were assumed for Mars flyby mission (600 to 700 days) and high energy for Venus. The years 1978 and 1980 were considered for Mars; 1980 for Venus.

Lunar Transfer Mission

A typical lunar transfer mission consists of the following major phases; boost out of Earth parking orbit, propulsive midcourse velocity correction, and a propulsive retro into a lunar orbit. Additional vehicle weight requirements are computed for life support expendables, propellant boil off, and attitude control. A 70-hour transfer trajectory was assumed for apogee, perigee, and mean transfer trajectories.

Orbital Altitudes

The following altitudes were assumed for the planetary and lunar circular orbits for computing the vehicle velocity and trajectory requirements.

The orbital altitude above the Earth's surface is 500 km for all Mars and Venus stopover and flyby missions. The orbital altitude for the circular orbits about Mars and Venus is 600 km. The Earth orbit altitude for lunar missions is 485 km; a 100 nm circular orbit altitude is used for the moon. The peripassage planet radius for all flyby missions is 1. 05 times the radius of the planet.

NUCLEAR ENGINE

Configuration

The study was confined to analysis and evaluation of beryllium-reflected graphite-moderated nuclear rocket engines. Both topping and bleed cycle engines and single and counterflow tie rod cooling were to be investigated. The reactor core diameters studied range from 45 to 65 in. in diameter.

Performance

The specific impulse varies parametrically from 700 to 900 seconds and the thrust from 50,000 to 500,000 pounds (approximately 1,000 to 12,000 Mw).

Engine Clustering

In order to increase the gross effective thrust and thereby reduce the velocity gravity losses, engine clustering, or the simultaneous use of two or more identical nuclear engines on a single stage, is used. Nuclear engine clustering is employed only for the depart Earth stage. As an alternative mode, aftercooling of the nuclear engine for later restart is assumed possible for the braking propulsion phase at the target planet.

Engine Weight

The preliminary weights of the nuclear engines used in the computations of vehicle weights are shown in Table II-1 as a function of the thrust per engine and number of clustered engines. More accurate engine weights were later generated with the NOP program. These engine weights include the weight of the reactor, pressure vessel, nozzle, shielding, reflector, feed system, thrust structure, and auxiliary engine components. The weight penalties associated with the clustering of engines for a given stage is based on data obtained from Aerojet General Corporation.

VEHICLE CONFIGURATION AND DESIGN

Vehicle and Mission Criteria

The major payload and vehicle performance criteria are summarized in Table II-2.

Table II-1 Nuclear Engine Weight

Thrust - lbs. No Engines Clustered	NUCLEAR ENGINE WEIGHT - LBS						
	50,000	100,000	200,000	230,000	300,000	400,000	500,000
Single	15,000	18,300	31,000	34,200	40,800	48,800	56,000
2	31,560	39,256	64,780	71,200	84,400	100,000	114,800
3	50,550	63,075	102,225	111,900	131,820	155,850	177,450
4	72,800	91,200	144,600	157,600	184,900	217,500	246,600
5	--	--	--	200,000	--	--	--
7	134,400	168,700	264,075	--	335,860	394,100	446,250

Minimum Vehicle Weight

Evaluation of the mission is based primarily on the total spacecraft weight. This weight is the minimum gross spacecraft weight that is required to perform a specified mission. This weight corresponds to the overall vehicle weight at the point just prior to boost out of Earth parking orbit. The vehicle weight in all cases is computed using trajectory characteristics that are optimum for the selected constraints.

In determining the vehicle configuration, its requirements, and its operation, no detailed considerations are given to the problems and require-ments of ascent to orbit and orbital rendezvous, assembly, checkout, and propellant and personnel transfer. Therefore, the vehicle primarily is sized and configured for the mission phases and operations commencing with boost out of an Earth parking orbit and terminating with Earth recovery or retro into lunar orbit.

Payloads

The payloads for all planetary flyby and stopover missions include 1) an Earth recovered module, 2) a mission module jettisoned prior to Earth entry, and 3) a planet lander or probe jettisoned at the target planet. In addition, in the stopover mission, an ascent module is picked up before leaving the target planet. The payload for the lunar mission is a parametric, inert weight delivered into lunar orbit. The payload weights are reasonable values obtained from the many interplanetary mission studies performed by NASA and industry in the past three years.

Table II-2

NOMINAL MISSION CRITERIA

GENERAL

Specific Impulse

Nuclear - 800 sec

Cryogenic Chemical (LO_2/LH_2) - 440 sec

Storable Chemical - 330 sec

Attitude Control

1 percent each leg

Micrometeoroid Protection

Optimum Cryogenic Insulation/Boiloff

MARS STOPOVER MISSION CRITERIA

Earth Recovered Payload	- 10,000 lb
Mission Module (8 Man)	- 68,734 lb plus solar flare shield
Mars Lander (MEM)	- 80,000 lb
Weight Recovered from MEM	- 1,500 lb
Life Support Expendables	- 50 lb/day
Stopover Time	- 20 days
Midcourse Correction	- 100 m/sec each leg storable propellant

FLYBY MISSION CRITERIA

Earth Landed Payload	- 8,500 lb
Mission Module (3 Man)	- 65,000 lb including solar flare shield
Planet Probe	- 10,000 lb
Life Support Expendables	- 40 lb/day
Planet Passage Altitude	- Mars - 1000 km $(R_d = 1.3)$
	Venus - 1000 km $(R_d = 1.16)$
Midcourse Correction	- 200 m/sec outbound leg 300 m/sec inbound leg storable propellant

LUNAR TRANSFER MISSION CRITERIA

Payload in 100 nmi Lunar Orbit	- 100,000 to 400,000 lb
Midcourse Correction	- 30 m/sec storable propellant
Transfer Time	- 70 hr

Propellant Tank Weights

The derivation of the propellant tank weight scaling laws were based on data generated by Lockheed Missile and Space Company under NASA Contract, NAS8-9500, for the George C. Marshall Space Flight Center (Ref. 1). A modular approach is used in which all tanks clustered in any given stage are of the same capacity. The maximum capacity of each tank is set by the limitations imposed by the Saturn V booster and its launching equipment.

The scaling laws used to relate the weight of the propellant tanks to the total usable propellant weight and trip time are given below for various propellants and mission phases. Also included are the primary assumptions used in formulating these equations

Primary Assumptions

Except for the depart Earth phase, all equations for cryogenic propellant tanks do not contain the weight provisions required for tank insulation.

All equations include the weight provisions required for micro-meteoroid protection.

The equations for the depart Earth phase contain tank insulation and micrometeoroid weight provisions sufficient for 90 days.

The equations for hydrogen propellant tanks do not include the nuclear engine weight, the engine shielding, or the thrust structure.

The equations for all chemical propellant tanks (non-nuclear) include the required engine weight. The engine, structure, and accessories have been sized to maintain a constant thrust-to-initial stage weight ratio of approximately 0.7.

The following define the nomenclature used in the scaling law equations:

W_{pmax}	-	The maximum usable propellant capacity for a single tank module
W_j	-	Final tank or stage jettison weight; total empty stage weight including propellant residuals (lbs)
W_p	-	Usable propellant weight (lbs)
T	-	Total time exposed to micrometeoroids (days)

<u>Depart Earth Stage</u> - LH_2 - 33 ft dia.

W_{pmax} ~ 342,540 lbs

$W_j = 0.1644 W_p + 6420$

<u>Depart Earth Stage</u> - LO_2/LH_2 - 33 ft. dia (common bulkhead)

W_{pmax} ~ 1,540,000 lbs

$W_j = 0.0485 W_p + 18,564$

<u>Arrive Planet and Depart Planet Stage</u> - LH_2 - 33 ft. dia

W_{pmax} ~ 342,540 lbs

$W_j = 0.12 W_p + 0.01492 T^{1/3} (0.02577 W_p + 493)^{4/3} + 8368$

<u>Arrive Planet and Depart Planet Stage</u> - LO_2/LH_2 - 21.67 ft. dia (common bulkhead)

W_{pmax} ~ 700,000 lbs

$W_j = 0.0469 W_p + 0.01492 T^{1/3} (0.01021 W_p - 104)^{4/3} + 11,904$

<u>Depart Planet Stage</u> - N_2O_4/A-50 - 21.67 ft. dia (separate tandem tanks)

W_{pmax} ~ 800,000 lbs

$W_j = 0.0284 W_p + 0.01492 T^{1/3} (0.0027 W_p + 1374)^{4/3} + 12,646$

<u>Arrive Earth Retro Stage</u> - LO_2/LH_2 - 21.67 ft. dia (internal tanks)

W_{pmax} ~ 150,000 lbs

$W_j = 0.0855 W_p + 0.01492 T^{1/3} (0.0186 W_p + 972)^{4/3} + 2865$

<u>Arrive Earth Retro Stage</u> - N_2O_4/A-50 - 21.67 ft. dia (internal tanks)

W_{pmax} ~ 150,000 lbs

$W_j = 0.0427 W_p + 0.01492 T^{1/3} (0.00595 W_p + 505)^{1/3} + 3094$

<u>Outbound Leg Midcourse Correction and Planet Capture Orbit Circularizing Stage</u> - N_2O_4/A-50 - 21.67 ft. dia (internal tanks)

W_{pmax} ~ 100,000 lbs

$w_j = 0.1154 W_p + 0.0259 T^{1/3} (0.00656 W_p + 489)^{4/3} + 1190$

Inbound Leg Midcourse Correction Stage - N_2O_4/A-50 - 21.67 ft. dia
(internal tanks)

W_{pmax} - 25,000 lbs

$W_j = 0.0665 W_p + 937$

Four additional classes or "levels" of scaling laws were used in portions of the study to define the various propellant tank jettison weights or mass fractions (ratio of total usable propellant to total gross stage weight). These are designated as mass fraction case numbers 1 through 4. The average mass fraction given by these four sets of scaling laws are listed in Table II-3 for the various propulsive modes the mission phases. The equations and average mass fractions for the nuclear stages do not include the weight of the nuclear engine.

Table II-3 Propellant Tank Mass Fractions

Stage Type	Average Mass Fraction			
	No. 1	No. 2	No. 3	No. 4
Nuclear (LH_2) Leave Earth	.88	.84	.80	.76
Nuclear (LH_2) 200 Day Storage	.87	.83	.79	.75
Cryogenic (LO_2/LH_2) Leave Earth	.94	.90	.86	.82
Cryogenic (LO_2/LH_2) 200 Day Storage	.92	.87	.82	.77 — No speculation
Storable 200 Day Storage	.95	.91	.87	.83
Cryogenic (LO_2/LH_2) Earth Retro	.79	.74	.69	.64 — No speculation
Storable Earth Retro	.91	.87	.83	.79

Earth Aerodynamic Braking

The range of aerodynamic braking capability at Earth to be investigated was assumed to vary parametrically from all aerodynamic braking to aerodynamic braking from parabolic entry velocity. The scaling laws for sizing the required structure, ablative material, insulation, and landing and recovery aids for aerodynamic braking are based on results generated by TRW/STL under NASA Contract NAS2-1409 for Ames Research Center.

The gross vehicle weight (including payload) or reentry module weight required for Earth aerodynamic braking is given by the following equation for a recovered or payload weight of 10,000 pounds. Analogous equations were used for the range of recovered weights from 7000 to 20,000 pounds.

$$W_{ERM} = 46.71 \, V_{AE}^{2} - 1043.3 \, V_{AE} + 20,122$$

where

W_{ERM} - Gross vehicle weight or Earth reentry module weight (lbs)

V_{AE} - Vehicle arrival velocity with respect to a non-rotating earth at an altitude of 100 km (km/sec)

Mars Aerodynamic Braking

Aerodynamic braking at Mars was considered as an alternative braking mode. It was assumed that the vehicle is aerodynamically braked into a capture orbit about Mars, after which the orbit is circularized by a storable propellant stage. The scaling law used to size the Mars aerodynamic braking heat shield is based on data obtained from Lewis Research Center.

The ratio of the heat shield weight to gross vehicle weight required for Mars aerodynamic braking is given by the following equation. The heat shield weight includes all expendable or jettisonable ablative material, structure, and insulation.

$$\frac{W_{S}}{W_{AM}} = K \, (0.001385 \, V_{AM}^{2} + 0.183)$$

where

W_{S} - Heat shield weight (lbs)

W_{AM} - Gross vehicle weight arriving at Mars (lbs)

V_{AM} - Vehicle arrival velocity with respect to Mars at an altitude of 167 km (km/sec)

K - Arbitrary constant used to vary scaling law parametrically. A value of $K = 1$ is used unless specifically noted.

Solar Flare Shielding

The solar flare shield weight is sized and the perihelion distance determined so as to have a minimum effect on the initial vehicle weight. The dependence of the solar flare shield scaling law on perihelion distance permits this optimization. The scaling law is based in part on data obtained from Lewis Research Center.

The scaling law equations shown below were used only for the vehicle weight computations for stopover missions. The solar flare shield weight for flyby missions is assumed constant and is included as part of the mission module weight.

Active Solar Flare Activity

$$W_S = 12,672 + \frac{2615}{r_p - 0.27165}$$

Intermediate Solar Flare Activity

$$W_S = 14,463 + \frac{1315}{r_p - 0.27085}$$

Quiet Solar Flare Activity

$$W_S = 16,266 + \frac{0.01}{r_p - 0.3}$$

The years 1980, 1982, and 1990 were considered as active years, the years 1978, 1984, and 1988 as intermediate years; and 1975 and 1986 as quiet years.

Non-Nuclear Propulsion Systems

In addition to the use of nuclear rocket engines for performing all of the major velocity changes, the use of nuclear and chemical engines in separate stages for the same mission, and all chemically propelled vehicles are also considered for evaluation and comparison purposes. Once a chemical stage is introduced into a particular mission (ignoring midcourse corrections), all remaining stages employ chemical propulsion. Separate chemical engines and stages are used for braking at and departing the target planet.

Both high energy cryogenic (LO_2/LH_2) and liquid storable chemical propulsion systems are considered with specific impulses of 440 sec and 330 sec, respectively.

Gravity Losses

The initial vehicle weight data are based on calculations for the propellant weight in which the velocity losses due to operation in a gravity field are taken into account in an exact manner. For vehicles employing nuclear propulsion stages, these losses are based on the required velocity change, the engine specific impulse, and the vehicle thrust-to-weight ratio obtained from the computed vehicle weight and the specified engine thrust.

For vehicles employing chemical propulsion systems, the characteristic velocity is obtained by increasing the required impulsive velocity change by a fixed percentage. The percentage values used are shown in the following schedule.

Propulsive Phase	Propulsion Mode	Percentage Increase
Depart Earth	Cryogenic (LO_2/LH_2)	2.3%
Arrive Planet	Cryogenic (LO_2/LH_2)	0 %
Depart Planet	Cryogenic (LO_2/LH_2)	1 %
Depart Planet	Storable	1 %
Arrive Earth Retro	Cryogenic (LO_2/LH_2)	0 %
Arrive Earth Retro	Storable	0 %

Cryogenic Propellant Storage

The computed initial vehicle weight includes the weight of the propellant tank insulation and vaporized propellant. These are determined in an optimum manner which considers the length of storage time and the various propulsive velocity changes that each cryogenic stage undergoes.

III MISSION OPTIMIZATION PROGRAMS

GENERAL

Within a given class of trajectories for any interplanetary flight, there usually exists one trajectory which requires the least initial vehicle weight to perform the mission. The optimization procedure developed for finding this trajectory is based on a mission in which the vehicle is given a relatively high thrust velocity change followed by a long coast or free flight period. Since a free flight trajectory is independent of the vehicle size and weight, it is not necessary to calculate continually new trajectory parameters for the optimization procedure. Rather, a trajectory map is generated and stored within the computer program for continual reference.

The initial version of the Stopover Mission Optimization Program (SMOP) stored the trajectory data as curve fits. For each arrive planet date (at fixed 10-day intervals over a specified range of arrive planet dates) the leave Earth and arrive planet characteristic velocities as a function of the outbound trip time, were fitted by 3rd order polynomials. The leave planet and arrive Earth characteristic velocities and the perihelion distance were also fitted by 3rd order polynomials, but as a function of the inbound trip time for each depart planet date.

To find the optimum trajectory and the minimum vehicle weight, the curve fits were used in outbound and inbound trip time optimization equations to find the optimum trip times and the corresponding velocities for each arrive planet date. With these data, the total vehicle weight for each arrive planet date was calculated, using the vehicle scaling laws, payloads, etc. listed in the previous chapter. The arrive planet date corresponding to the minimum vehicle weight was found by curve fitting the three smallest vehicle weights as a function of the arrive planet date, differentiating the equation, and setting it equal to zero.

This procedure required a large number of passes through the vehicle weight calculation procedure. Also, it was very troublesome developing 3rd order curve fits of the velocities and perihelion distance that were sufficiently accurate over the trip time range of interest. (This general procedure was retained and used for the FLyby Optimization Program (FLOP) since curve fitting of the trajectory data was not necessary. A description of this procedure is given in this chapter.)

When the requirement was imposed to develop an optimization program for swingby missions, it was clear that attempting to optimize the mission by extending the initial SMOP procedure would be very cumbersome and costly in computer time. The powered swingby has one more independent trajectory parameter, which adds another dimension to the trajectory map on the swingby portion of the mission. This added dimension would have complicated the trajectory data curve fitting and increased the number of passes through the vehicle weight calculation portion of the program. Therefore, a basic change in the method of trajectory data storage and arrive planet date optimization was made.

The trajectory map is stored in the SWingby Optimization Program (SWOP) as discrete values of the dependent parameters at regular intervals of the independent parameters. No curve fit preprocessing is necessary. The curve fitting is done internally to the program, using 2nd order polynomials. Rather than calculating the initial vehicle weight for the stopover mission and unpowered swingby mission for each arrive planet date to find the minimum vehicle weight, one weight calculation is made and an optimization equation used to determine the optimum arrive planet date. The optimum outbound and inbound leg times, as before are found using optimization equations. For a powered swingby mission, an additional optimization equation is used to find the optimum third leg time. The computer time required per case has remained about the same, but now it is much easier to prepare the trajectory data for the program, and the program has the potential to handle increasingly complicated mission.

In order to accurately account for the velocity losses due to finite firing time in a gravity field, the impulsive velocity data stored in the program are corrected for this effect by multiplying the velocities by gravity loss factors to obtain the characteristic velocity change. The gravity loss factors are stored in the program as a function of specific impulse, thrust-to-weight ratio, and impulsive velocity. They were obtained by simulating powered flights for leaving Earth, and arriving and leaving the target planet.

FLYBY MISSION

Only two independent trajectory parameters are needed to completely define a flyby mission. However, if the constraint of constant periplanet distance is imposed for a series of possible flights, only one independent parameter is left to specify. The FLyby Optimization Program (FLOP) uses the arrive planet date as the independent parameter. No trajectory curve fits are used. The dependent leave and arrive Earth velocities and outbound and inbound leg times are supplied to the program at uniform intervals of the arrive planet date. The flyby trajectory data used for this study was supplied by MSFC.

The flyby mission optimization procedure is shown in Fig. III-1. The overall optimization is divided into two parts. First, the initial vehicle weight is calculated for each arrive planet date over a range of dates that are specified by input. Starting with the arrive Earth payload, the program works backward to the initial vehicle weight using the correct leave Earth gravity loss factors and the scaling laws, payloads, and co-efficients described previously. The calculations for the leave Earth stage are repeated until consistent values of the initial weight in Earth orbit (thrust-to-weight ratio) and the velocity gravity loss is obtained.

Second, once the initial vehicle weights for the range of arrive planet dates are obtained, the three lightest vehicle weights are curve fitted as a function of the arrive planet date. By differentiating the curve fit, the arrive planet date corresponding to the minimum weight vehicle is found. Then all trajectory parameters for this "optimum" arrive planet date are found by curve fitting the stored trajectory data. The vehicle component weights and auxiliary output quantities are then determined for the optimum date (and corresponding optimum velocities) by passing through the weight calculation portion of the program once more. The equations and detail procedures employed in FLOP are completely outlined in the program documentation, Vol. VIII, of this series of final reports.
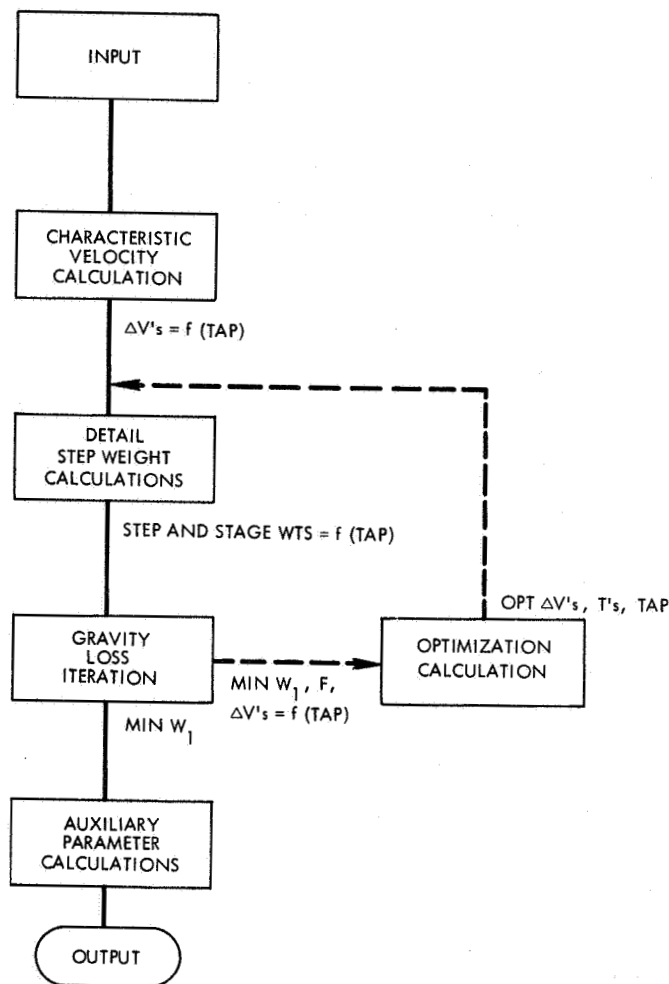
Figure III-1 Flyby Mission Optimization Procedure

STOPOVER AND SWINGBY MISSIONS

Generalized Mission Analysis Procedure

The mission analysis for the stopover and swingby missions is split into two parts, a trajectory optimization and a vehicle weight calculation. Each part supplies the other with necessary trajectory or vehicle parameters. Figure III-2 shows the generalized mission analysis procedure employed by the SWingby Optimization Program (SWOP). This procedure is applicable to the optimization of stopover missions and both powered and unpowered, turn inbound and outbound, swingby missions.
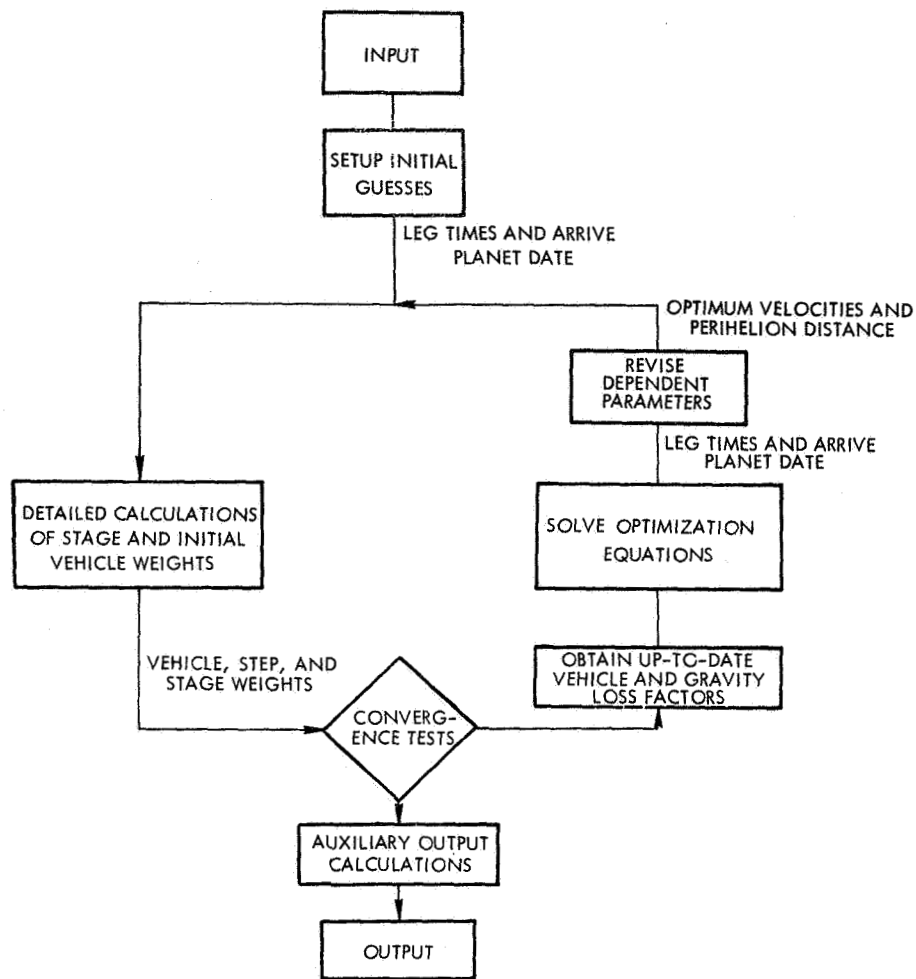
Figure III-2 Swingby Mission Optimization Procedure

The necessary scaling law coefficients and vehicle constraints are inputted and then initial guesses for the independent trajectory parameters are used to start a mission optimization. The stored trajectory data are used to determine the characteristic velocities corresponding to these initial guesses. Then a detailed calculation of the vehicle stage weights is made and the resulting vehicle stage weights are combined with calculated velocity gravity losses to form coefficients in the optimization equations. The optimization equations are then solved for the "optimum" leg times and arrive planet date. The characteristic velocities and perihelion distance corresponding to these "optimum" independent parameters are obtained from stored trajectory data.

These new values of velocities and perihelion distance are used in re-calculating the stage and initial vehicle weights. When a sufficient number of interations are performed successive new values of vehicle weights and trajectory parameters no longer appreciably change. At that time, the calculated vehicle weights satisfy convergence tests and the computational procedure is terminated following the computation of required auxiliary output values. The pertinent mission, vehicle, and performance data are obtained on a three page printout.

Trajectory Data

Stopover and Unpowered Swingby Missions - The stopover and unpowered swingby missions require three independent parameters to completely specify their trajectory. The three independent parameters used in this study are the arrive planet date and the outbound and inbound leg times. This selection permits all of the dependent trajectory parameters (leave and arrive Earth velocities, arrive and leave target planet velocities, and the perihelion distance for the stopover mission, plus periplanet distance and the third leg time for the swingby mission) to be expressed as functions of only two of these independent trajectory parameters. This greatly eases the problems associated with the generation and storage of trajectory data. In addition, the leg time optimization equations are simplified.

In generating the stopover trajectory data, the inbound and outbound legs are treated separately by selecting either an arrive planet or a depart planet date. A discrete set of outbound or inbound trip times are then considered, and the dependent velocities and perihelion distances obtained by free flight trajectory simulations as a function of the trip time, for the fixed arrive or depart date. For this arrive or depart date, the range of trip times that contains all possible optimum trajectories can be determined and the data within this range are processed for storage. The arrive planet or depart planet date is then changed by a uniform interval, and the process repeated for another set of trip times. In this manner, an entire set of maps of the dependent variables as functions of the independent parameters are obtained. The stopover trajectory data used in this study were taken from Ref. 2 as well as generated at TRW/STL.

Powered Swingby Mission - The powered turn swingby mission introduces two additional degrees of freedom to the trajectory specifications. However, it has been shown (Ref. 3) that there is an optimum relationship between the periplanet distance, PP, and the impulsive velocity change, VI, when passing the swingby planet. This relationship can be used while generating the trajectory data to obtain the optimum combination of PP and VI. If the optimum PP is less than the minimum pass distance, PPMIN, for any particular set of independent parameters, PP must be set equal to PPMIN and the corresponding VI calculated. Using this set of values results in only one new degree of freedom. The parameter selected as the additional independent parameter is the third leg time, which may be the leg time between Earth and the swingby planet for an outbound swingby and between the swingby planet and Earth for an inbound swingby.

The powered swingby trajectory data are generated much the same as for the stopover mission. For an inbound swingby, the depart planet date is set, the inbound leg time to the swingby planet is set, and the third leg time is then varied over a discrete set of values. The leave planet, optimum swingby, and arrive Earth velocities, the optimum periplanet distance, and the perihelion distance, are obtained as a function of the third leg time for the fixed planet date and inbound leg time. If PP < PPMIN, the VI corresponding to PPMIN is obtained.

The inbound leg time is then changed by a uniform interval, and the process repeated for another range of third leg times. This is continued over the desired inbound leg time range. The leave planet date is then incremented, and the entire process repeated for another inbound leg time range, and more third leg time ranges.

Since no consistent set of powered swingby trajectory data was available it was not possible to analyze any powered swingby missions during the study although the powered swingby option of SWOP program is fully developed.

Derivation of Optimization Equations

There are several sets of optimization equations for the different combinations of stopover missions and powered and unpowered turn, inbound and outbound, swingby missions. In addition, different forms of the equations result when certain constraints are imposed, such as a specified or constrained total trip time. The equations for all missions are listed in Vol. III of this series of final reports.

For summarization purposes, the optimization equations are derived for the inbound powered turn swingby mission. For this mission, there are four independent parameters. These are the outbound trip time, TO, the arrive planet date, TAP, the first inbound leg time, TI1, and the second inbound leg time, TI2. If the vehicle payload ratio is PLR = $W_{initial}/W_{final}$, the minimum vehicle weight (or maximum payload) occurs when

$$d(PLR) = \frac{\partial(PLR)}{\partial(TO)} d(TO) + \frac{\partial(PLR)}{\partial(TAP)} d(TAP) + \frac{\partial(PLR)}{\partial(TI1)} d(TI1)$$

$$+ \frac{\partial(PLR)}{\partial(TI2)} d(TI2) \tag{1}$$

$$= 0$$

or when

$$\frac{\partial(PLR)}{\partial(TO)} = 0 \tag{2}$$

$$\frac{\partial(PLR)}{\partial(TAP)} = 0 \tag{3}$$

$$\frac{\partial(PLR)}{\partial(TI1)} = 0 \tag{4}$$

$$\frac{\partial(PLR)}{\partial(TI2)} = 0 \tag{5}$$

Equations 2 to 5 must all equal zero simultaneously to satisfy Eq. 1.

The first step in deriving the four optimization equations is to set up the payload ratio equation, which defines the entire vehicle as a function of the trajectory parameters and vehicle constants.

The dependent trajectory parameters which affect the vehicle weight are the five major velocity changes and the perihelion distance, r_p, which are functions of two or three of the four independent trajectory parameters, TO, TAP, TI1, and TI2. The functional dependence of these parameters is

$$VLE = f(TO, TAP)$$
$$VAP = f(TO, TAP)$$
$$VLP = f(TDP, TI1)$$
$$VI = f(TDP, TI1, TI2)$$
$$VAE = f(TDP, TI1, TI2)$$
$$r_p = f(TDP, TI1, TI2)$$

where the depart planet date, TDP, is simply related to the arrive planet date, TAP, by the stopover time, TSO.

The jettison weight of each stage of the vehicle is represented by the structure factor, obtained from the vehicle weight calculation. Using the various stage structure factors, the inputted payload values, the solar flare shielding weight scaling law, and the time dependent weights such as vaporizing propellant and life support expendables, the payload ratio equation can be constructed as a function of the independent and dependent parameters.

$$PLR = f(VLE, VAP, VLP, VI, r_p, VAE, TO, TI) \tag{6}$$

The optimization equations are obtained by differentiating Eq. 6 with respect to each of the four independent trajectory parameters (Eqs. 2 to 5).

As an example, the outbound trip time optimization equation (Eq. 2) takes the form

$$\frac{\partial PLR}{\partial TO} = \frac{\partial PLR}{\partial VLE} \frac{\partial VLE}{\partial TO} + \frac{\partial PLR}{\partial VAP} \frac{\partial VAP}{\partial TO} + \frac{\partial PLR}{\partial TO} \tag{7}$$

$$= K_1 \frac{\partial VLE}{\partial TO} + K_2 \frac{\partial VAP}{\partial TO} + K_3$$

$$= 0$$

where the constants, K_1, K_2, and K_3 are the weight derivatives or vehicle exchange ratios. These constants have a relatively simple form and are a function of inputted and calculated weight data. The partial derivatives of the trajectory parameters are obtained by two or three dimensional curve fitting of the stored trajectory data with 2nd order polynomials. The curve fit for each dependent parameter is made as a function of the applicable independent parameter. The values of the other three independent parameters are held constant at the inputted best estimates or at the values obtained from the previous iteration. As an example (Fig. III-3) the curve fit for VLE for a constant arrive planet date (TAP) is

$$VLE = A_{LE} (TO)^2 + B_{LE} TO + C_{LE} \tag{8}$$

The curve fit for VAP yields a similar expression.

III-9
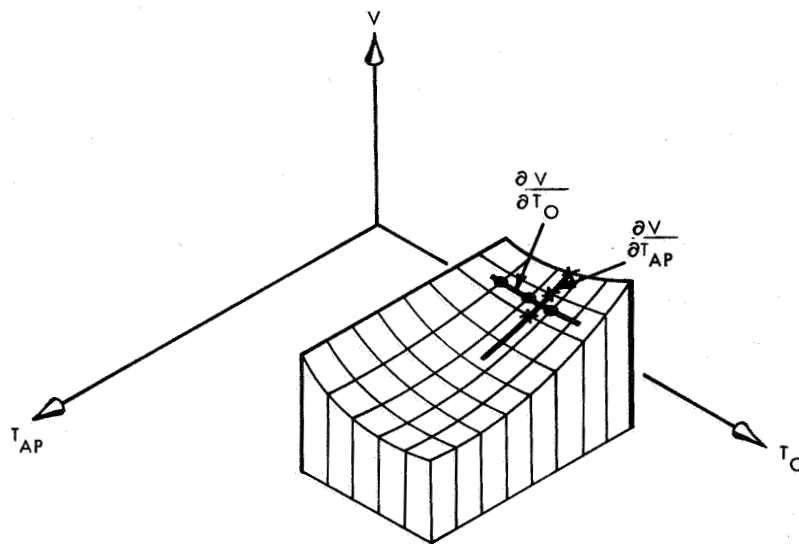
FINDING PARTIAL DERIVATIVES FROM STORED DATA
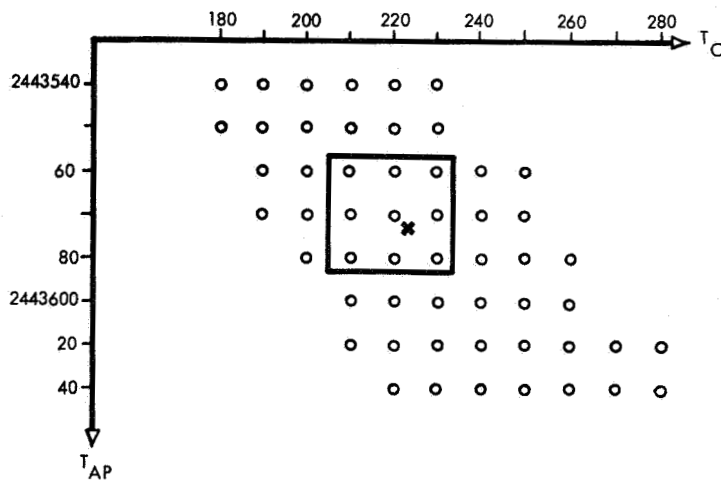
PLAN VIEW OF STORED TRAJECTORY DATA

Figure III-3   Stored Trajectory Data

Substituting the values of the weight derivatives and velocity derivatives into Eq. 7 permits the solution for the optimum outbound trip time.

$$TO = \frac{-\left[K_1 \, B_{LE} + K_2 \, B_{AP} + K_3\right]}{2\left[K_1 \, A_{LE} + K_2 \, A_{AP}\right]} \tag{9}$$

III-10

Similarly, the solutions of the remaining three optimization equations (Eqs. 3, 4, and 5) yield the optimum values of the remaining three independent parameters. The stored trajectory data can then be used to determine the velocities and perihelion distance corresponding to the optimum independent parameters.

The derivation and solution of the optimization equations for the other types of missions are accomplished in an analogous manner.

Optimization of Missions with Constraints on Independent Parameters

It is possible to constrain any or all of the independent trajectory parameters, as well as any of the related parameters, such as the leave Earth date. For the four independent trajectory parameters, this is done simply by not solving the optimization equation corresponding to the constrained parameter. For a constraint on the leave or arrive Earth date, the arrive planet date optimization equation is not solved, and the arrive planet date is set equal to either the leave Earth date plus the outbound time or the arrive Earth date minus the inbound and stopover time.

A constraint on the total trip time is harder to handle. This reduces the number of independent parameters by one and requires a revision of one leg time optimization equation and the elimination of another. The relationship between the total trip time and the leg time is used in the solution of the revised optimization equation.

IV   ENGINE OPTIMIZATION PROGRAM

ENGINE DESCRIPTION

The nuclear rocket engines investigated during the course of this study were beryllium-reflected, graphite-moderated, nuclear rocket engines employing a hot bleed turbine cycle or a topping turbine cycle. The schematic diagram, presented as Fig. IV-1 shows the major engine subsystem and the propellant flow pattern for a typical nuclear engine using a hot bleed cycle. The major components of a solid core nuclear rocket engine include the graphite-moderated and uranium carbide-fueled reactor core, interface region, beryllium reflector, core support plate, tie rods, radiation shield, pressure vessel, nozzle, propellant lines, pump, turbine, thrust structure, thrust vector control system, tank valve assembly, roll control system , diagnostic instrumentation system, pneumatic system, destruct system, and control system.
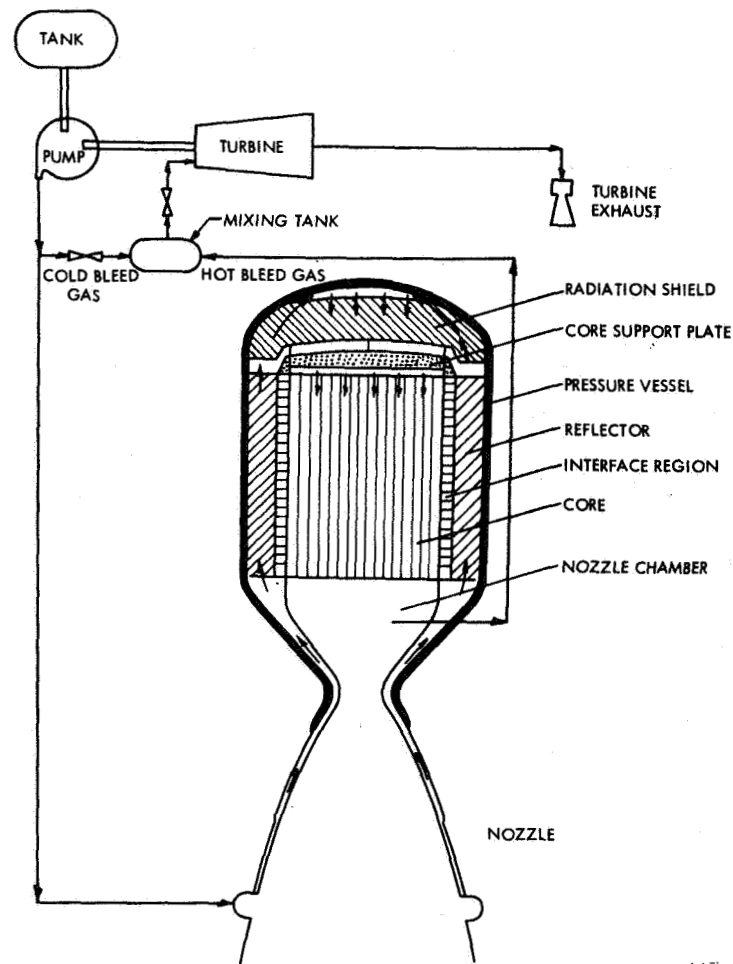

Figure IV-1 Propellant Flow Diagram-Bleed Cycle

The propellant is stored in the propellant tank as cryogenic hydrogen at a temperature of about 37° R and a pressure of 25 psia. The liquid hydrogen is forced through an axial or centrifugal pump which discharges the high pressure hydrogen into the pump discharge line. The hydrogen at a pressure of about 1000 psia enters the nozzle torus. At this point, the hydrogen flow may be split with a portion of the hydrogen regeneratively cooling the nozzle throat section while the remaining hydrogen may be used to cool a portion of the divergent section between the torus and skirt or nozzle exit. The hydrogen experiences about a 150 to 200 psi pressure drop and a 50 to 100°R temperature rise in maintaining the hot-side nozzle wall temperature below about 2000° R.

The high pressure hydrogen cools the interface region, reflector, radiation shield, and core support plate. These regions of the reactor experience significant radiation heating due to the nuclear radiation generated in the reactor core. The propellant temperature and pressure at the core inlet is typically 200° R and 700 psia. The propellant then flows through coolant channels in the graphite reactor core where it is heated to exit gas temperatures of 4000° R to 5000° R.

For engines with single-pass tie tubes, a portion of the propellant passing through the reactor core is diverted into the tie tubes to maintain the desired tie rod temperatures. The relatively cool tie tube coolant is discharged into the nozzle chamber and mixed with the hot gas discharged from the "fueled" coolant channels. For double-pass tie tubes, a small quantity of cold gas is extracted at the pump discharge and passed through the tie tube. The tie tube coolant is discharged at the core inlet and then passes through coolant channels in the reactor core.

After emerging from the reactor core, the hot hydrogen is expanded through a converging/diverging nozzle. A small fraction of hot gas is bled from the nozzle chamber, diluted with colder hydrogen, and used to drive the bleed turbine. The turbine exhaust is then passed through an auxiliary nozzle for thrust recovery.

The propellant flow scheme and major engine subsystems of a representative nuclear rocket engine employing a topping turbine cycle are presented schematically in Fig. IV-2.
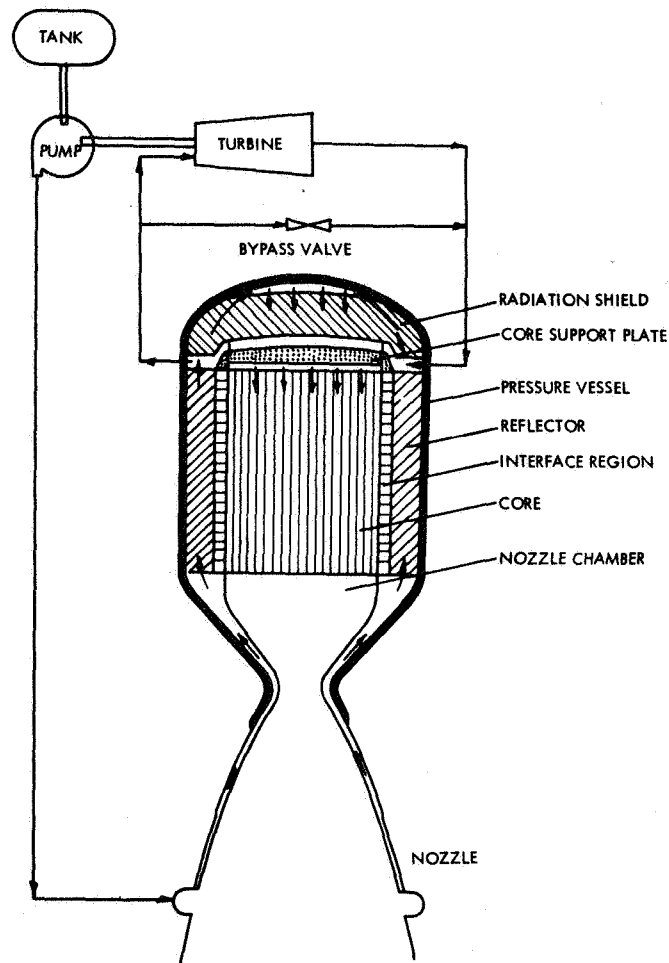
Figure IV-2 Propellant Flow Diagram-Topping Cycle

In the topping cycle, the propellant is heated in the reflector and interface region by nuclear radiation heating and by an auxiliary heat source (preheater) contained in either, or both , of these regions. The heated propellant, in part or totally, is passed through a topping turbine. The turbine exhaust then flows through the radiation shield and core support plate before entering the reactor core. The topping cycle produces a higher specific impulse for the same chamber temperature, since no propellant is exhausted through an auxiliary

nozzle with an accompanying reduction in specific impulse. However, the increased complexity of the topping cycle and the greater coupling of the reactor and feed system complicates the control of such engines and somewhat detracts from the topping cycle's apparent performance advantage.

ENGINE ANALYSIS TECHNIQUES

The influence of the principal engine design parameters and constraints on engine performance was evaluated utilizing a digital computer program developed during the study. This preliminary engine analysis program, the Nuclear Rocket Engine Optimization Program (NOP), conducts a rapid parametric analysis of beryllium-reflected, graphite-moderated nuclear rocket engines. The engine analysis determines the engine design characteristics and engine weight based on specified engine performance (i.e., specific impulse and engine power or thrust), cycle type, and design constraints. These design contraints are imposed by nuclear, thermal, and structural limitations. The basic program inputs and outputs are illustrated schematically in Fig. IV-3.

INPUTS ─────────────────────────────┐
     SPECIFIC IMPULSE
     POWER
     FUEL ELEMENT CONFIGURATION
      AND CONSTRAINTS
     CORE DESIGN CRITERIA
     ENGINE CYCLE AND FEED
      SYSTEM PARAMETERS

          NOP

     OPTIMUM ENGINE WEIGHT AND
     OPTIMUM ENGINE THRUST
      AS FUNCTIONS OF
       SPECIFIC IMPULSE
       POWER
     PRELIMINARY OPTIMUM ENGINE DESIGN
      REACTOR CORE DETAIL
      REFLECTOR, PRESSURE SHELL, NOZZLE,
      FEED SYSTEM REQUIREMENTS
     SPECTRUM OF OFF-OPTIMUM DESIGNS

                                 OUTPUTS
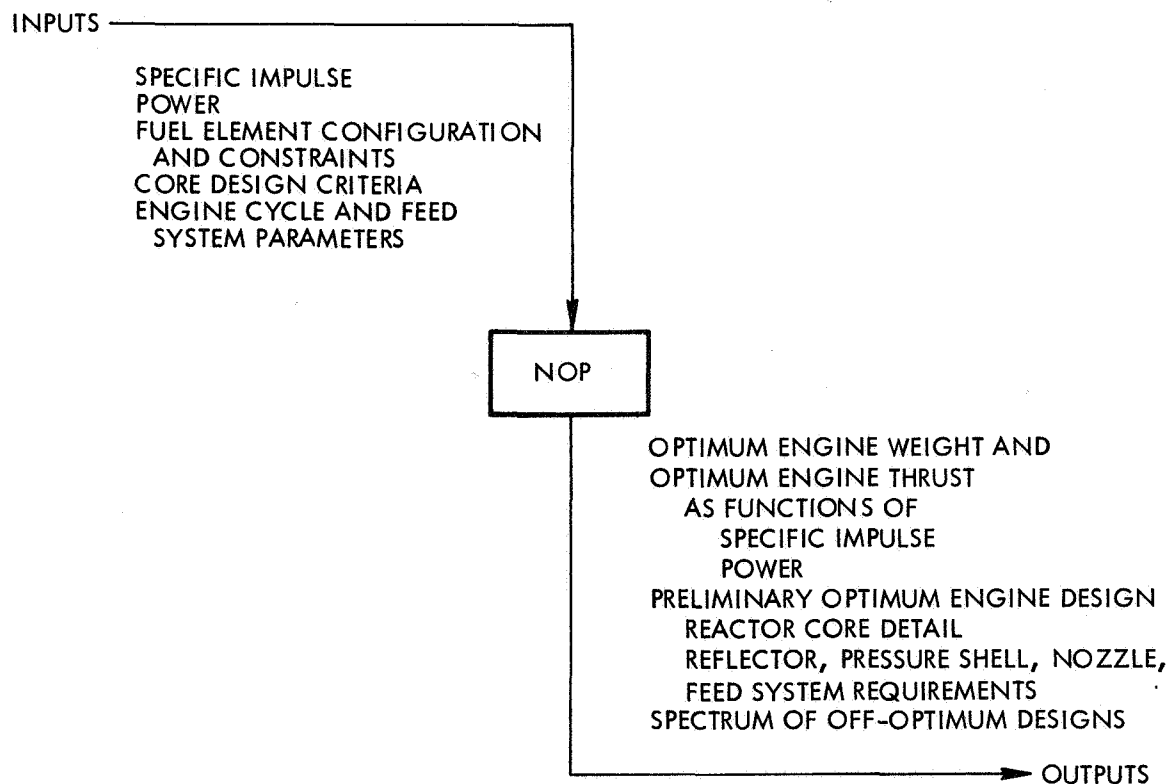
Figure IV-3 NOP Basic Inputs and Outputs

The program strives to preserve the accuracy of more detailed differential calculations through the use of integral relationships. The integral correlations were derived from the fundamental differential equations and, thus, retain the correct functional dependence on the basic physical parameters. The correlations and scaling laws used by the program were normalized and compared with detailed nuclear, thermal, and shielding analyses and in some instances, normalized to experimental results.

The program is capable of evaluating an array of engine cycle types which include the hot bleed cycle, partial topping cycle, and full topping cycle. Different fuel and support element geometrics can be analyzed along with different component materials for the interface region, core support plate, radiation shield, nozzle, pressure vessel, and propellant line assemblies. The weight scaling laws for the auxiliary engine components such as the pneumatic system, diagnostic instrumentation, thrust structure, etc., are in the form of quadratic polynomials with coefficients which can be normalized to detailed component designs. In addition, turbo pump weights corresponding to single units or multiple units can be specified.

The digital computer program conducts an engine analysis, shown schematically in Fig. IV-4, which is composed of the following nine major subanalyses: the core thermal analysis; reactor criticality analysis; support plate mechanical and thermal analysis; propellant heating, propellant shielding, and radiation shield thermal analysis; reflector and interface region thermal analysis; propellant feed system analysis; engine weight analysis; and aftercooling analysis. In order to briefly indicate the scope and detail of the analysis, a brief description of the calculational sequence used in NOP is presented in the following paragraphs.

Input

In order to initiate an engine calculation, the desired engine performance (specific impulse and reactor power), engine description, and engine design constraints must be specified.
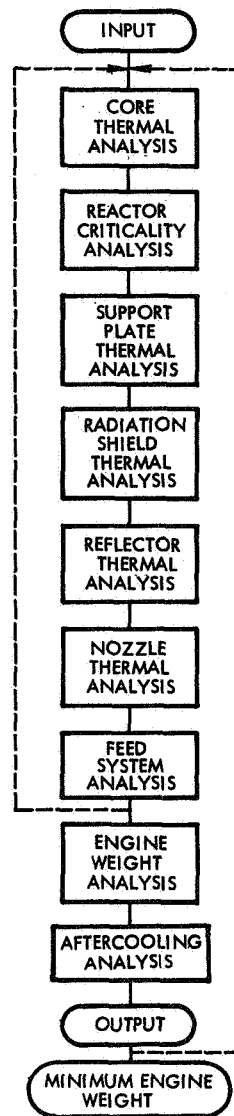
Figure IV-4   NOP Calculational Sequence

For each combination of specific impulse and reactor power (thrust), the program selects a specified combination of main nozzle expansion ratio, nozzle chamber pressure, core pressure drop, and coolant channel diameter. For the selected combination of engine variables, the program calculates the engine weight required to produce the specified engine performance.

Core Thermal Analysis

Initially, the program assumes a turbine bleed fraction and knowing the average engine specific impulse and auxiliary nozzle specific impulse, the program calculates the main nozzle specific impulse. Since the main nozzle expansion ratio, nozzle efficiency, and chamber pressure are known, the mixed mean chamber temperature is calculated. By assuming a core inlet temperature,

the program iteratively solves for the fueled channel outlet temperature, support element solid fraction, and the bleed fraction required for cooling the support elements. The maximum core power density can then be determined for the coolant channel generating peak power. For the specified coolant channel diameter and core pressure drop, the program solves the momentum and energy equations for the coolant channel length and coolant mass flow rate per unit area. Next, the peak fuel temperature, core solid fraction, and power per unit of core area are determined. The program then computes the core radius required to produce the specified core power. At this point in the calculational sequence, the core thermal analysis has sized the reactor core entirely from thermal considerations.

Reactor Criticality Analysis

The program next evaluates the fuel loading required for criticality and to achieve the desired shutdown reactivity. The next step is to size the beryllium reflector to provide sufficient excess reactivity for control purposes.

Support Plate, Radiation Shield, and Reflector Thermal Analysis

The core support plate thickness is calculated based on mechanical deflection criteria. The radiation heating in the support plate is computed and the propellant properties upstream of the support plate are evaluated. The radiation shield thickness is calculated based on the allowable radiation energy flux which can be incident on the hydrogen in the propellant tank. The propellant temperature rise and pressure drop across the radiation shield, and the radiation heating in the reflector and interface region are computed. The reflector and interface region propellant pressure drop and temperature rise are also evaluated.

Nozzle Thermal Analysis

The nozzle throat dimensions and the heat flux at the nozzle throat are determined. The program then evaluates the coolant-side propellant temperature rise, the nozzle coolant tube diameter, and the coolant-side pressure drop.

Feed System Analysis

At this stage of the calculation, the turbine work, pump work, and pump inlet temperature are computed. The pump inlet temperature can now be matched to the tank temperature by varying the reactor inlet temperature. The pump work and turbine work are compared and, if they are not compatible, a new bleed fraction is estimated and the entire computational loop is repeated until agreement is obtained.

Engine Weight Analysis

The weights of the engine components are calculated and summed to yield the total engine weight for the selected engine constraints and engine variables of interest. After completing this sequence of calculations, the program has determined a consistent engine design, and the engine description, engine dimensions, propellant properties, and component weights are presented as output. The program then proceeds to a new combination of engine variables and performs another engine analysis.

Output

For each set of engine input parameters, the program computes a consistent preliminary engine design and outputs the most relevant quantities characterizing the design. These quantities include the engine performance, component description, component dimensions, component weights, and propellant characteristics at various locations throughout the system. For each combination of performance parameters, the program searches the engine designs generated, selects the minimum weight engine, and specifies the combination of engine variables producing the minimum engine weight. A preliminary engine design using the NOP program requires approximately 15 seconds of IBM 7094 computer time.

V MISSION ORIENTED NUCLEAR SYSTEM PARAMETERS EVALUATION RESULTS

The mission and engine optimization programs (SWOP, FLOP, and NOP) were employed, to evaluate a number of different missions, operational modes and ranges of engine design parameters and constraints. The evaluation results were used to determine the compromise engine and representative vehicle designs, establish the sensitivity of the vehicle weight to variations in engine, vehicle, and mission parameters, compare the advanced nuclear engine with chemical propulsive systems, and explore the utility of the advanced nuclear engine for various missions and vehicle types.

A summary of the major study results and conclusions obtained from these evaluations is given in this chapter. For a complete data background to the sections in this chapter, the reader is referred to Vols. II, III, and V.

INITIAL VEHICLE WEIGHT REQUIREMENTS

The initial vehicle weights required in Earth orbit in order to perform a wide variety of interplanetary missions for various operational and vehicle modes were established.

Figure V-1 compares the orbital launch weight requirements for four different propulsive and Mars aerodynamic braking mode combinations for Mars and Venus stopover missions.

For the Mars stopover mission and an Earth aerodynamic braking capability from 15 km per sec, the all nuclear propelled vehicle requires an orbital launch weight of 1.5 million pounds in 1986 and 4.3 to 5.0 million pounds in 1978. In contrast, the all cryogenic propellant (LO_2/LH_2) vehicle requires 4.0 million pounds in 1986 and upwards of 20 million pounds in 1978. If aerodynamic braking is employed for capture into Martian orbit, the nuclear vehicle weight is reduced to 1.2 million pounds in 1986 and 2.4 million pounds in 1978. The cryogenic vehicle weight reduces to 2.2 million pounds for 1986 and 5.0 to 6.0 million pounds in 1978.

The other Mars mission opportunities require vehicle weights between the extremes given above.

DEPART EARTH	ARRIVE MARS	DEPART MARS
NUCLEAR	AERO	NUCLEAR
CRYOGENIC	AERO	CRYOGENIC
NUCLEAR	NUCLEAR	NUCLEAR
CRYOGENIC	CRYOGENIC	CRYOGENIC

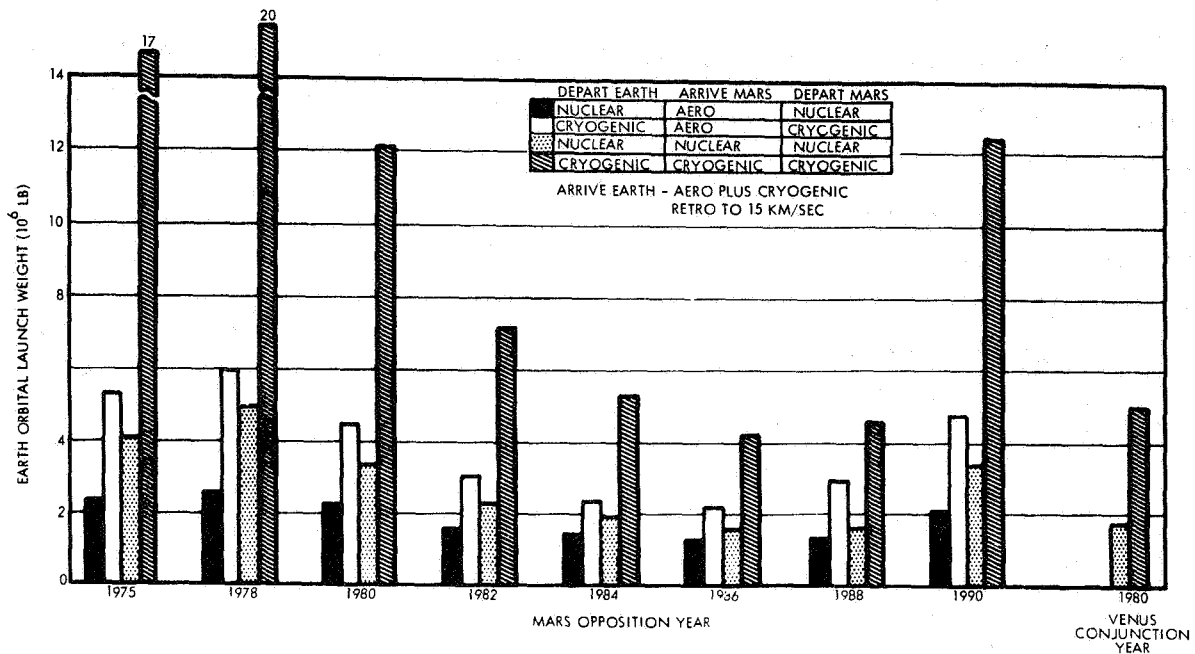ARRIVE EARTH - AERO PLUS CRYOGENIC
RETRO TO 15 KM/SEC

Figure V-1 Orbital Launch Weight Comparisons

Figure V-1 shows that the Venus stopover mission requires approximately 2.0 million pounds for the nuclear vehicle which is approximately equal to the 1986 Mars mission. The cryogenic propellant vehicle requires 5.0 to 6.0 million pounds and thus is similar to the 1984 Mars mission. These values only vary slightly among conjunction dates. In all cases, the Earth arrival velocity for the Venus mission is less than 15 km per sec and therefore, no retro stage is required for the assumed aerodynamic braking capability used in this figure.

The low energy, manned Mars flyby mission requires a nuclear vehicle weighing between 340,000 and 430,000 pounds depending on the nuclear engine thrust and Earth aerodynamic braking capability. The vehicle weight for a high energy Venus flyby mission will vary between 270,000 and 350,000 pounds again depending on thrust and aerodynamic braking capability.

A lunar transfer mission delivering a payload into lunar orbit requires vehicles weighing approximately 500,000 pounds for a 200,000-pound payload; 750,000 pounds for a 300,000-pound payload; and 950,000 pounds for a 400,000 pound payload.

NUCLEAR ENGINE THRUST REQUIREMENTS

The first step in the determination of an optimum nuclear engine was the selection of the compromise thrust level in order to narrow down the range of thrusts within which a more detailed analysis could be performed to directly relate the engine parameters to the mission performance.

The assumption was made that the selection of the optimum thrust range was relatively insensitive to the engine weight and specific impulse, and therefore, the nuclear engine specific impulse was held constant at 800 sec.

A large number of Mars and Venus stopover and flyby missions and lunar transfer missions were evaluated to determine the optimum thrust range for the nuclear engine. For any given mission, nuclear engines of the same thrust level were used to perform the required velocity changes for departing Earth, braking into Martian orbit, and departing Mars. Single engines were used for the Mars propulsion stages, while the number of engines for the depart Earth propulsion phase was varied from one to seven. Two other modes were investigated; in the first, the arrive Mars nuclear engine was aftercooled and reused for departing Mars. The second alternative mode employed a cryogenic stage (LO_2/LH_2) for departing Mars.

Figure V-2 is typical of the many graphs of the mission data. The initial vehicle weight in Earth orbit and the maximum firing time of any single nuclear engine is plotted as a function of the nuclear engine thrust and the number of engines in the leave Earth stage. From this and many other similar figures, the optimum thrust (minimum vehicle weight) could be determined for the many vehicle configurations, aerodynamic braking capabilities, and mission years investigated. The vehicle weight corresponding to this optimum thrust point was recorded from all of the data graphs and plotted against various parameters in order to determine the optimum thrust ranges and to analyze the influence of various parameters on the optimum thrust.

The optimum thrust point was selected in all cases consistent with the maximum nuclear engine firing time of 1800 sec for any single engine in the vehicle. This 1800-second firing time limitation is somewhat arbitrary, but represented a near optimum value from a mission performance standpoint.
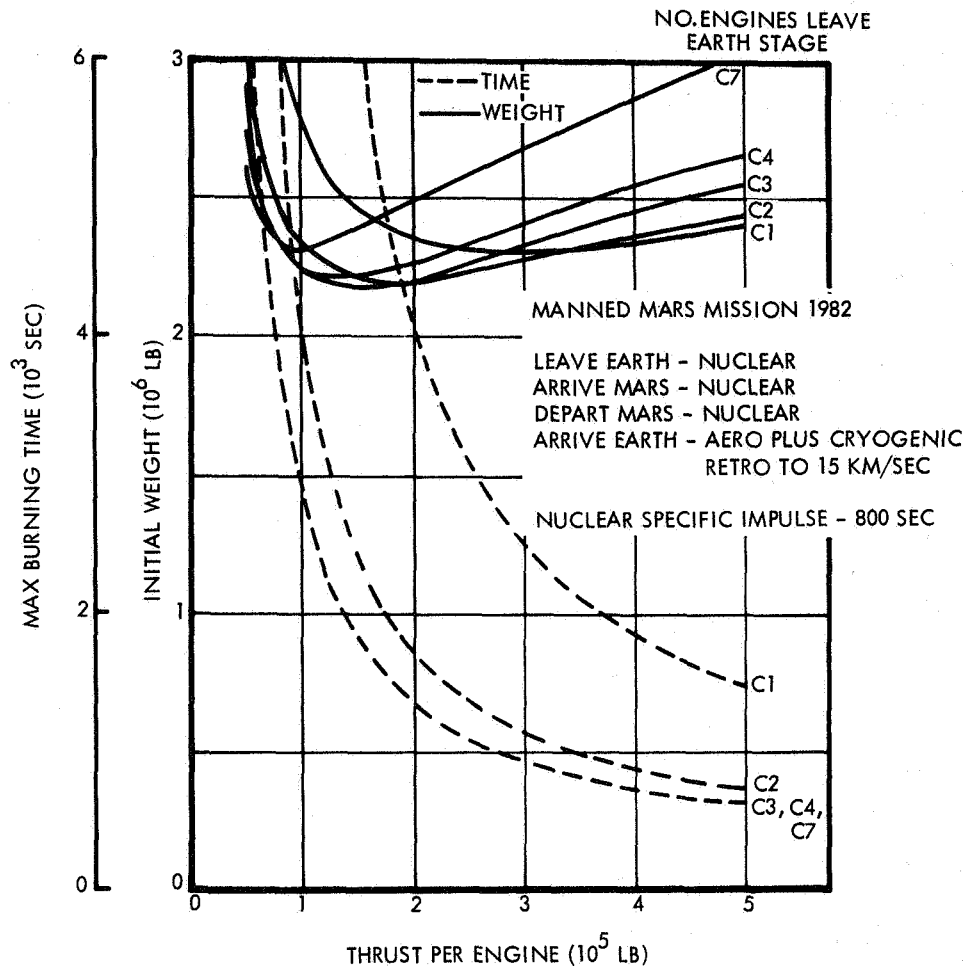
Figure V-2 Typical Mission Evaluation Result
Manned Mars Stopover Mission

When the limitation on maximum firing time is removed, the reduction in initial
vehicle weight is negligible, and the firing time corresponding to the optimum
thrust level does not exceed 2800 seconds except where aftercooling the arrive
Mars stage is used in which case the maximum total burn time for that engine
approaches 4000 sec.

The results indicate that the use of an aftercooled nuclear engine for the
Martian velocity changes requires approximately ten percent more initial vehicle
weight than for the nonaftercooled mode. This decided weight disadvantage of
the aftercooled mode favors the use of the nonaftercooled mode in all cases.

The use of a cryogenic propulsion stage for departing Mars increases the required vehicle weight by 20 to 30 percent over the all nuclear mode. Therefore, there appears to be no weight or operational factors that could justify the use of a chemical stage for departing Mars when nuclear engines are available and utilized for the other propulsive phases. In addition, the use of a storable arrive Earth retro stage leads to a lower performance vehicle than can be obtained with a cryogenic retro stage. The increased weight requirements for the storable propellant vary from 5 to 20 percent and are a direct function of the required retro velocity as well as the required velocity changes for the preceding mission phases.

In summary, no weight advantage is gained by using the aftercooling mode, the cryogenic (LO_2/LH_2) depart Mars mode, or a storable propellant for the arrive Earth retro stage.

Figure IV-3 compares, for the all nuclear nonaftercooled mode, three capabilities of Earth braking, all aerodynamic, and two modes in which a cryogenic retro is employed to decelerate the vehicle to 15 km per sec and parabolic velocities after which the vehicle enters the Earth's atmosphere aerodynamically.

This figure shows the sensitivity of the initial vehicle weight to the mission year and the Earth aerodynamic braking capability. For Earth retro braking to 15 km per sec, the vehicle weight for 1978 is over twice that required for 1986. In addition, the vehicle weight more than doubles for the extreme possibilities of Earth aerodynamic braking capability for both the years 1978 and 1982. These results indicate the sensitivity effect that is seen throughout all of these and the subsequent mission results. That is, the more difficult the mission or the less the vehicle performance capability, the greater the sensitivity of the vehicle weight to variations in any given parameter or mode.

The optimum thrust levels for the manned Mars vehicles are primarily a function of the vehicle weight. Therefore, it is to be expected that the optimum thrust requirements will vary widely throughout the range of mission years.

DEPART EARTH - NUCLEAR
ARRIVE MARS - NUCLEAR
DEPART MARS - NUCLEAR
ARRIVE EARTH -

■ AERO
□ AERO PLUS CRYOGENIC RETRO TO 15 KM/SEC
▨ AERO PLUS CRYOGENIC RETRO TO PARABOLIC VELOCITY

EARTH ORBITAL LAUNCH WEIGHT (10^6 LB)
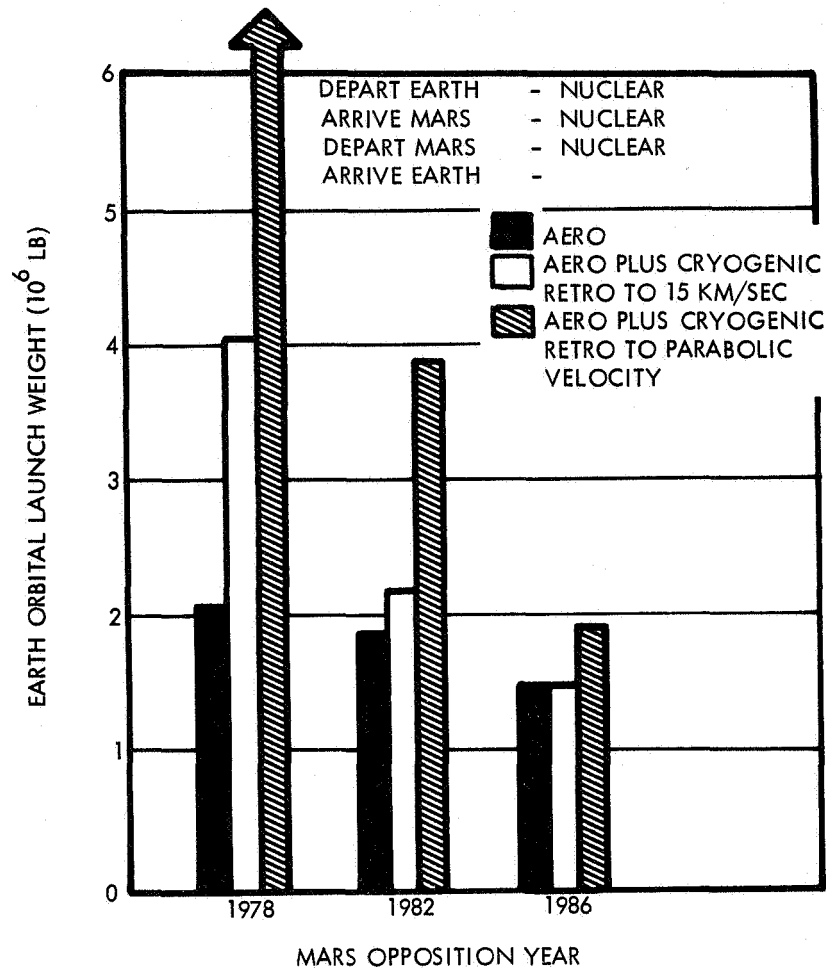
MARS OPPOSITION YEAR

Figure V-3 Orbital Launch Weights for Mars Stopover Missions

This variation is seen in Figure V-4, which is a composite of the many curves similar to Fig. V-2.

This figure shows the relationships that exist among the initial vehicle weight requirements, the thrust per engine, and the mission year. The discontinuities in the curves occur when an engine firing time of 1800 seconds is attained, at which point an additional nuclear engine is employed in a clustered arrangement to reduce the firing time for the leave Earth stage. As the engine thrust is further and further diminished, the firing time for the arrive Mars stage increases until the 1800-second limitation is exceeded. The curves are then drawn in dashed lines.
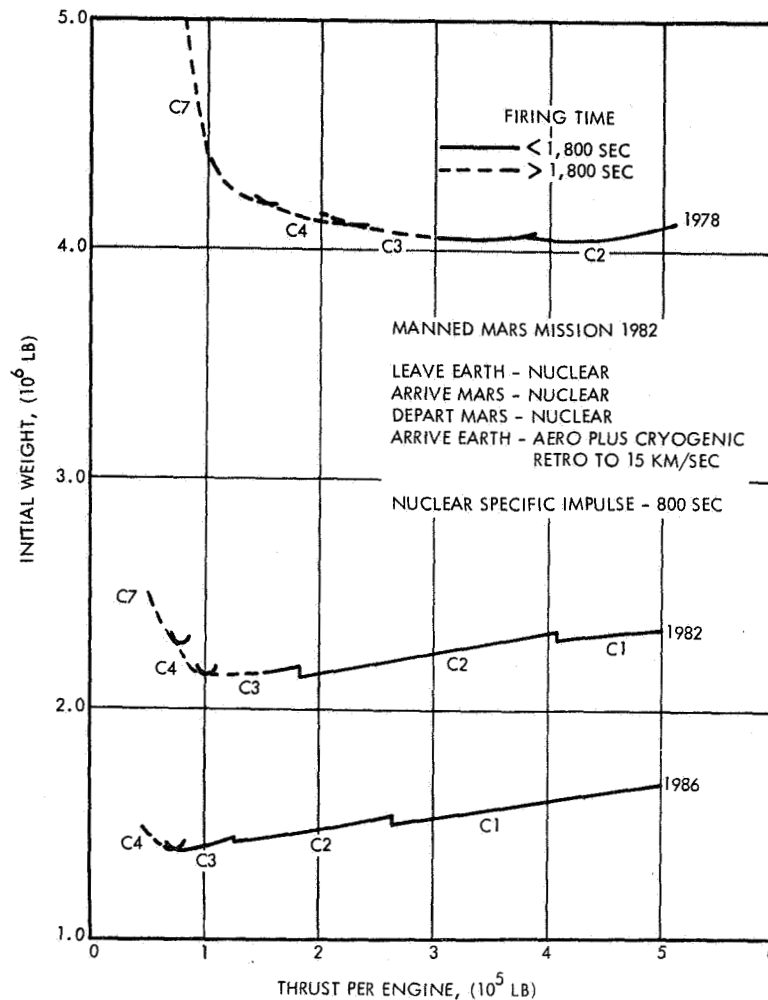
Figure V-4 Mars Stopover Mission-Nuclear Engine Thrust Requirements

For these typical Mars stopover missions, the optimum thrusts range from approximately 125,000 to 300,000 pounds.

System weight increases from the assumed nominal values can easily occur due to the uncertainty of environmental factors and future technological developments. Any increase in payload or system weights or decrease in performance will increase the vehicle weight, thus increasing the optimum thrust level. Furthermore, the vehicle weight is more sensitive to a decrease in thrust from the optimum value than for an increase in thrust. These two conditions tend to favor the selection of a compromise thrust that is greater than the midrange of the optimum values. An engine thrust between 200,000 and 250,000 pounds appears reasonable for the manned Mars stopover missions.

The compromise nuclear engine should also be capable of reasonable performance for departing Earth for planetary flyby and lunar logistic missions. The relationship between the optimum initial vehicle weight and engine thrust is presented in Fig. V-5 for these missions.
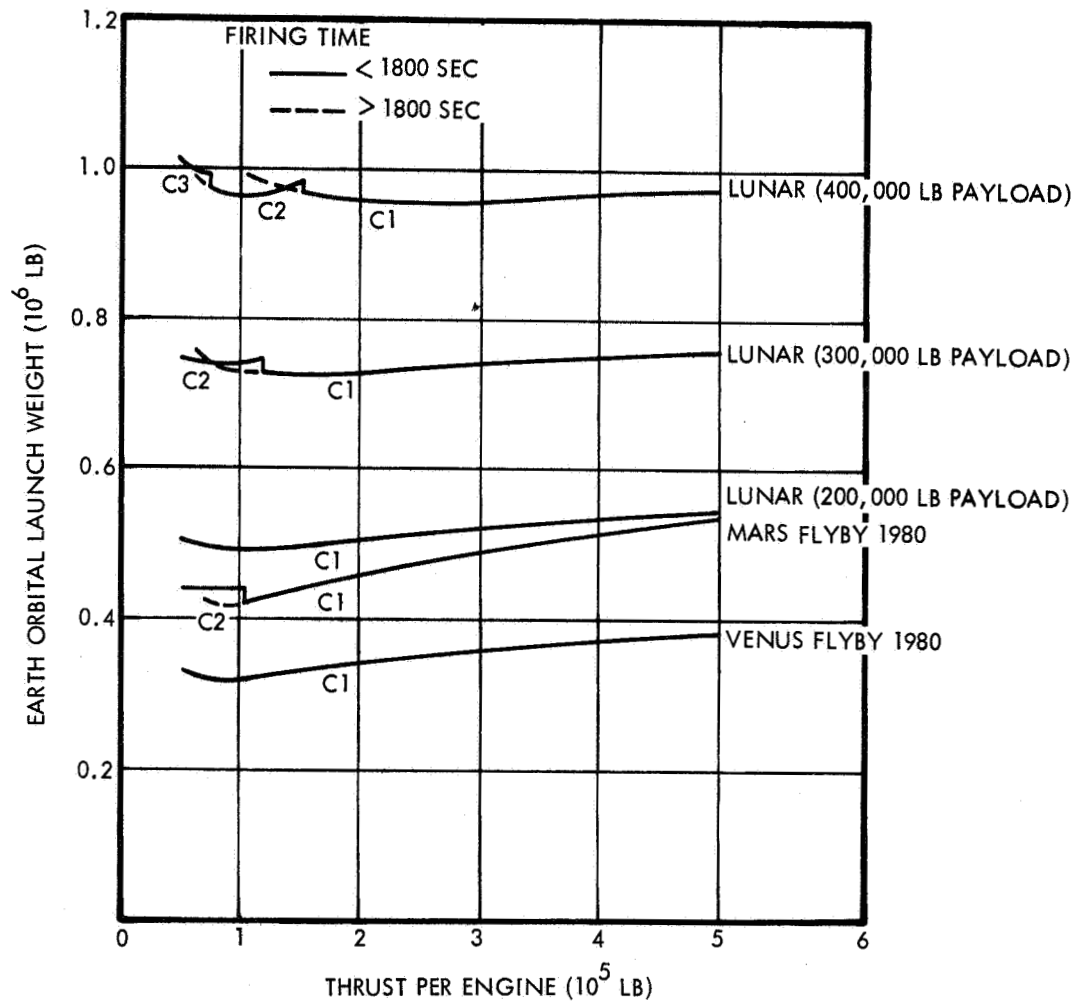

Figure V-5 Planetary Flyby and Lunar Missions - Nuclear Engine
Thrust Requirements

For the range of payloads shown, the vehicle performance for lunar missions is relatively insensitive to changes in engine thrusts from 50,000 to 400,000 pounds, if engine clustering is utilized. The 200,000 to 250,000-pound thrust range is nearly optimum for the larger lunar payloads, while the required vehicle weight is increased from the optimum by only four percent for the 200,000-pound payload.

The vehicle weight is slightly more sensitive to the engine thrust for flyby missions than for the lunar missions. Figure V-5 shows a maximum increase of eight percent in vehicle weight from the optimum when 200,000 to 250,000-pound thrust engines are used.

An approximate thrust of 230,000 pounds was selected by NASA as a nominal value for further mission and engine analysis. This selection reflects the results obtained in this study as well as the results of current technical effort on advanced nuclear engines being performed elsewhere.

INFLUENCE OF ENGINE PARAMETERS ON ENGINE PERFORMANCE

The sensitivity of vehicle weight to changes in engine design parameters may be obtained by initially finding the influence of each engine design parameter on engine performance, i.e., engine weight, specific impulse, and thrust. Then the influence of the engine performance on vehicle weight can be determined. The attainable engine performance, however, is highly dependent on the engine design constraints. The choice of these constraints requires considerable knowledge concerning engine technology and must be selected within developable limits.

Engine Performance Sensitivity

The sensitivity of nuclear engine performance to the principal engine design parameters and constraints was examined for minimum weight engines of the 200,000 to 250,000-pound thrust class. For each set of engine variables and constraints, the optimum length-to-diameter ratio was obtained by varying the core coolant channel diameter. A typical variation of engine weight as a function of specific impulse and coolant channel diameter is depicted in Fig. V-6.

Since the core pressure drop, reactor power, and power density are held constant, the optimum core coolant channel diameter defines the optimum core length-to-diameter ratio. For the range of core pressure drops and nozzle chamber pressures investigated, the core length-to-diameter ratios of minimum weight engines are shown in Fig. V-7 to range between 1.0 and 1.1. The higher values of length-to-diameter ratio correspond to higher specific impulses.
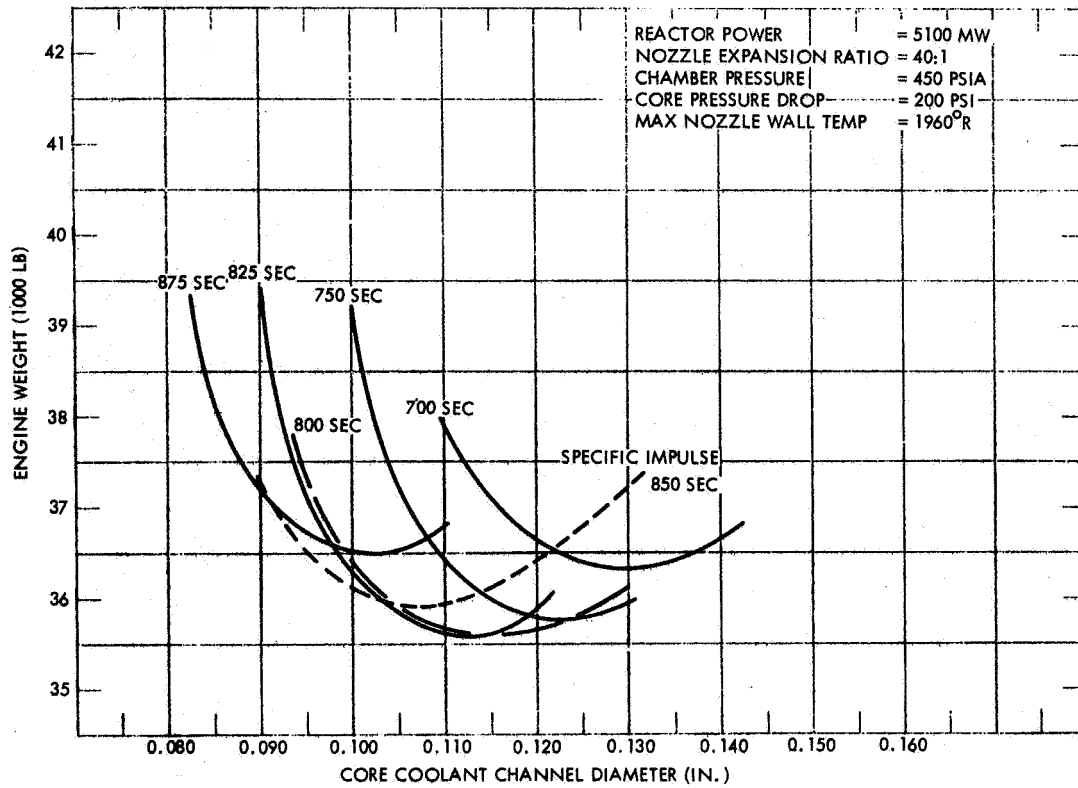
Figure V-6 Effect of Core Coolant Channel Diameter
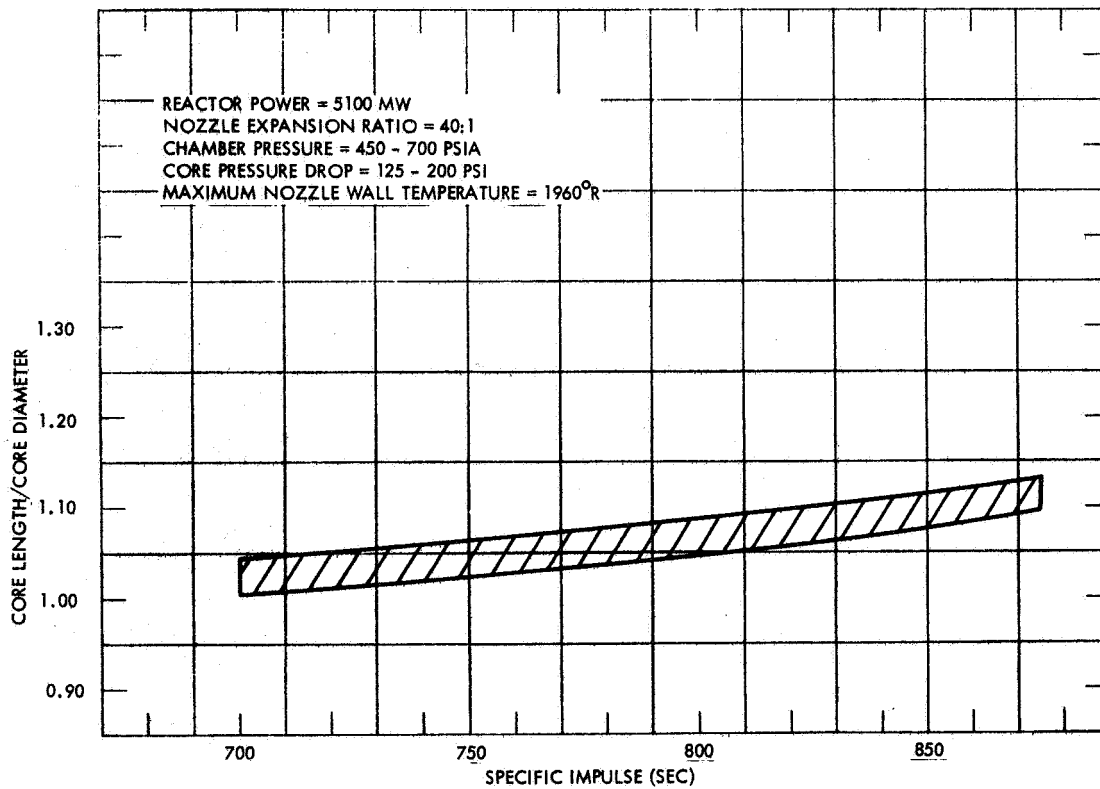and Specific Impulse on Engine Weight

Figure V-7 The Effect of Specific Impulse on Core
Length-to-Diameter Ratio

The effect of nozzle chamber pressure and specific impulse on minimum engine weight is shown in Fig. V-8. The influence of nozzle chamber pressure becomes increasingly important at higher specific impulses. Furthermore, for a particular nozzle chamber temperature, higher specific impulses are attainable at lower engine weights as the chamber pressure is reduced. The minimum engine weight increases for specific impulses less than 840 seconds if the chamber pressure is reduced below 450 psia. As the chamber pressure is decreased, a higher specific impulse is produced for a specified nozzle chamber temperature because of the decrease in the coolant-side nozzle pressure drop. The reduction in nozzle pressure drop means lower pump discharge pressures, and therefore, the lower turbine bleed fractions. Thus, for a bleed cycle engine, less propellant is exhausted through the auxiliary nozzle and the engine's performance is improved.
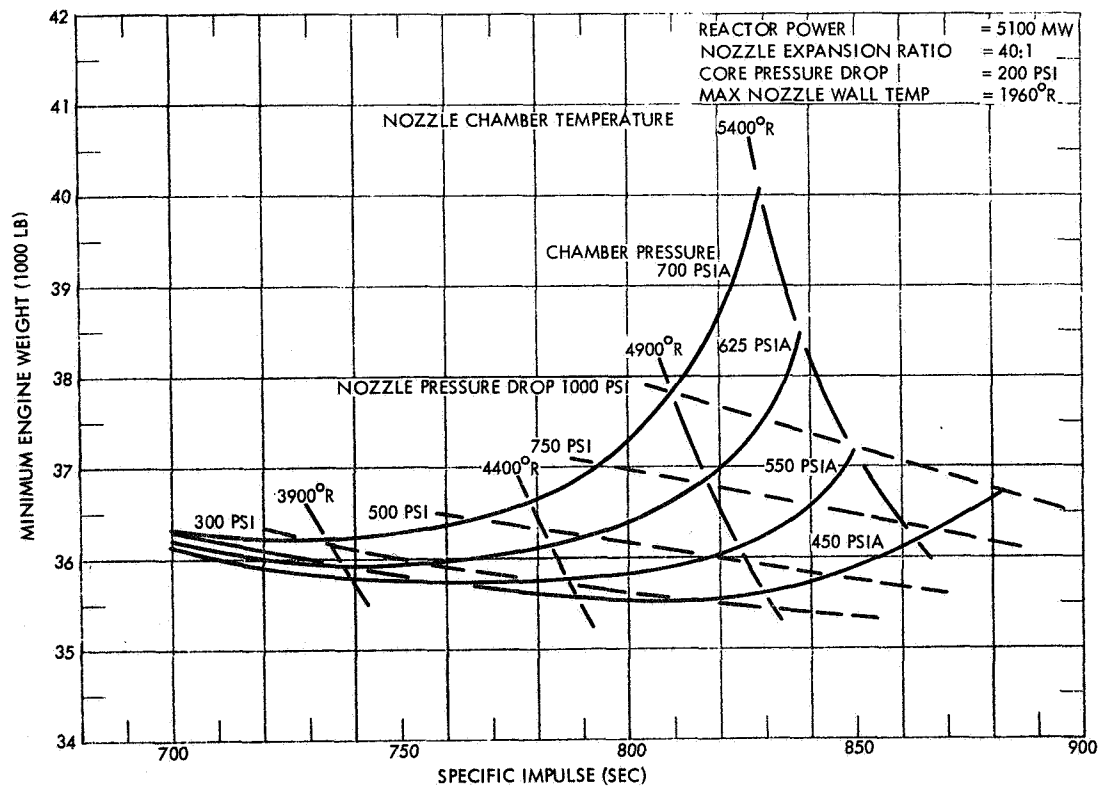

Figure V-8 Effect of Nozzle Chamber Pressure and
Specific Impulse on Minimum Engine Weight

The curves depicting the variation of minimum engine weight with chamber pressure and specific impulse are sensitive to the nozzle expansion ratio. For instance, an increase in nozzle expansion ratio from 40:1 to 120:1 shifts the curves approximately 100 seconds of specific impulse to the right. For engines with specific impulses of 800 to 850 seconds, nozzle chamber pressures of from 350 to 500 psia result in minimum weight engines.

The variation of engine thrust with specific impulse and chamber pressure is shown in Fig. V-9. At constant reactor power the engine thrust varies approximately as the inverse of specific impulse.
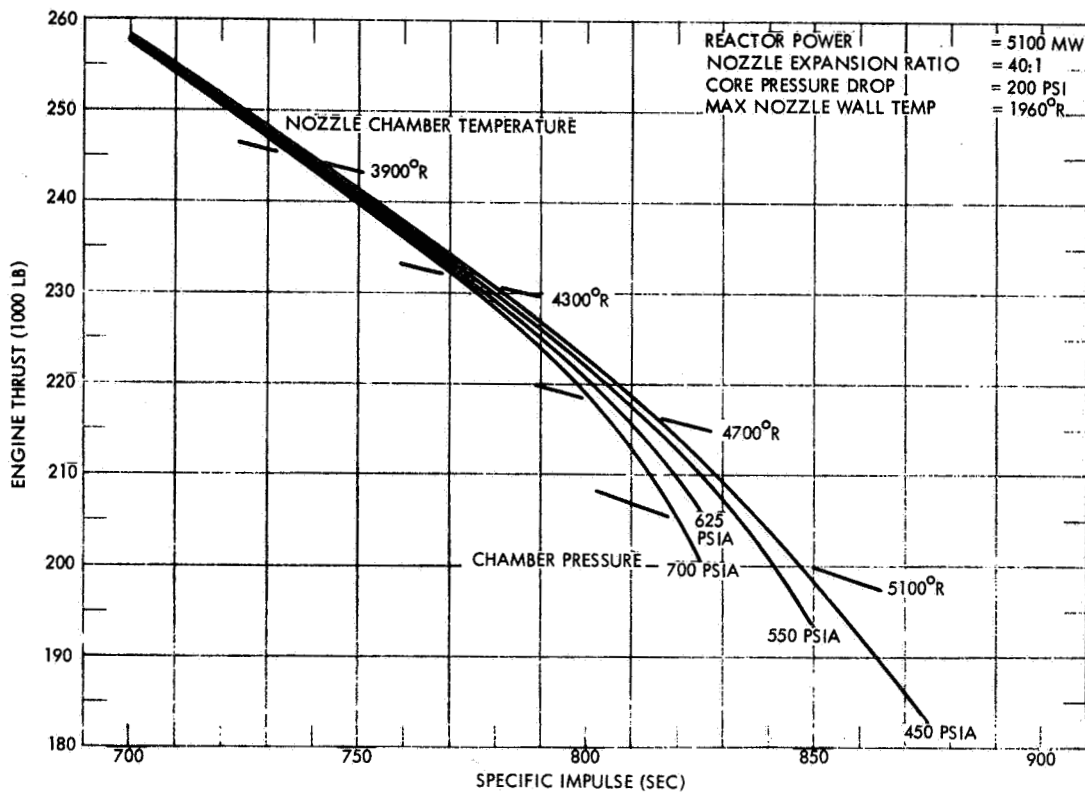

Figure V-9 Effect of Nozzle Chamber Pressure and
Specific Impulse on Engine Thrust

The influence of nozzle expansion ratio and specific impulse on the minimum engine weight is presented in Fig. V-10. For a fixed exit gas temperature, increasing the nozzle expansion ratio up to 120:1 produces a significant increase in specific impulse. Because larger nozzle expansion ratios also produce heavier engines, the apparent performance advantage associated with the higher specific impulse is diminished.
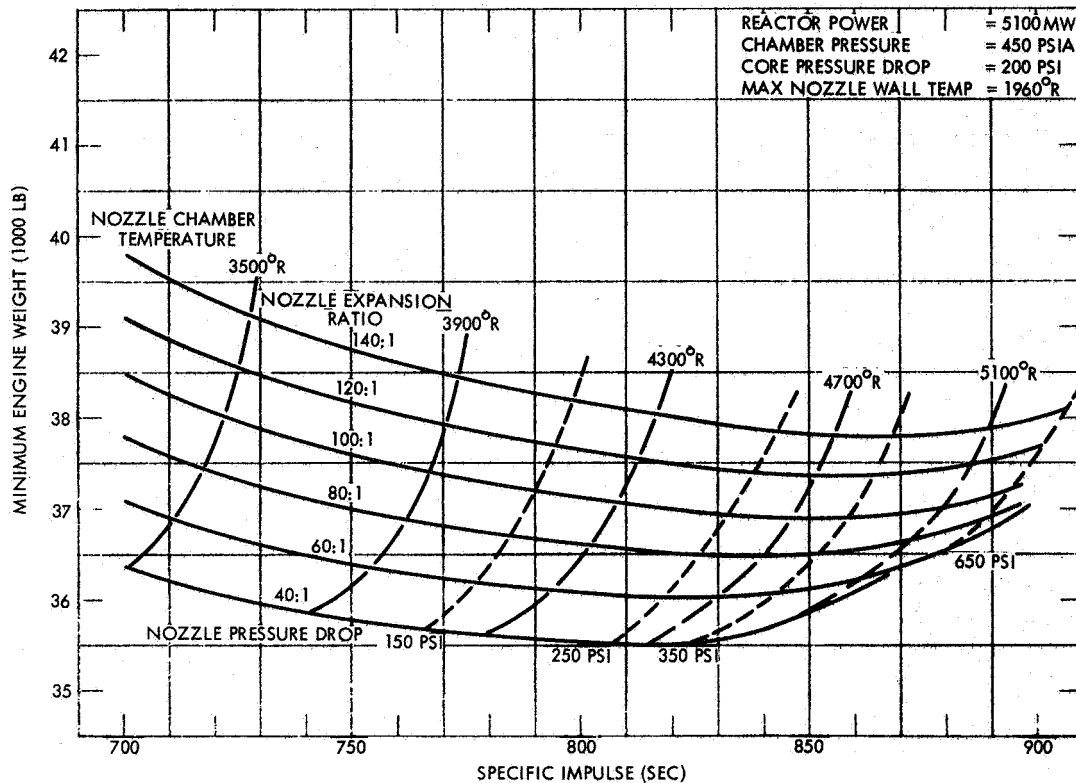
Figure V-10 Effect of Nozzle Expansion Ratio and
Specific Impulse on Minimum Engine Weight

The significant increase in engine thrust and specific impulse with an increase in nozzle expansion ratio is shown in Fig. V-11 for various nozzle chamber temperatures. For a constant nozzle chamber temperature or peak fuel temperature, an increase in nozzle expansion ratio from 40:1 to 140:1 increases both engine specific impulse and thrust. The variation in engine thrust for a given change in expansion ratio is relatively insensitive to the particular value of specific impulse.

The variation of minimum engine weight as a function of core pressure drop and specific impulse is shown by Fig. V-12. Increasing core pressure drop yields lower weight engines. The effect on minimum engine weight associated with increasing core pressure drop diminishes as core pressure drop increases. The core coolant channel diameter which produces the minimum engine weight decreases
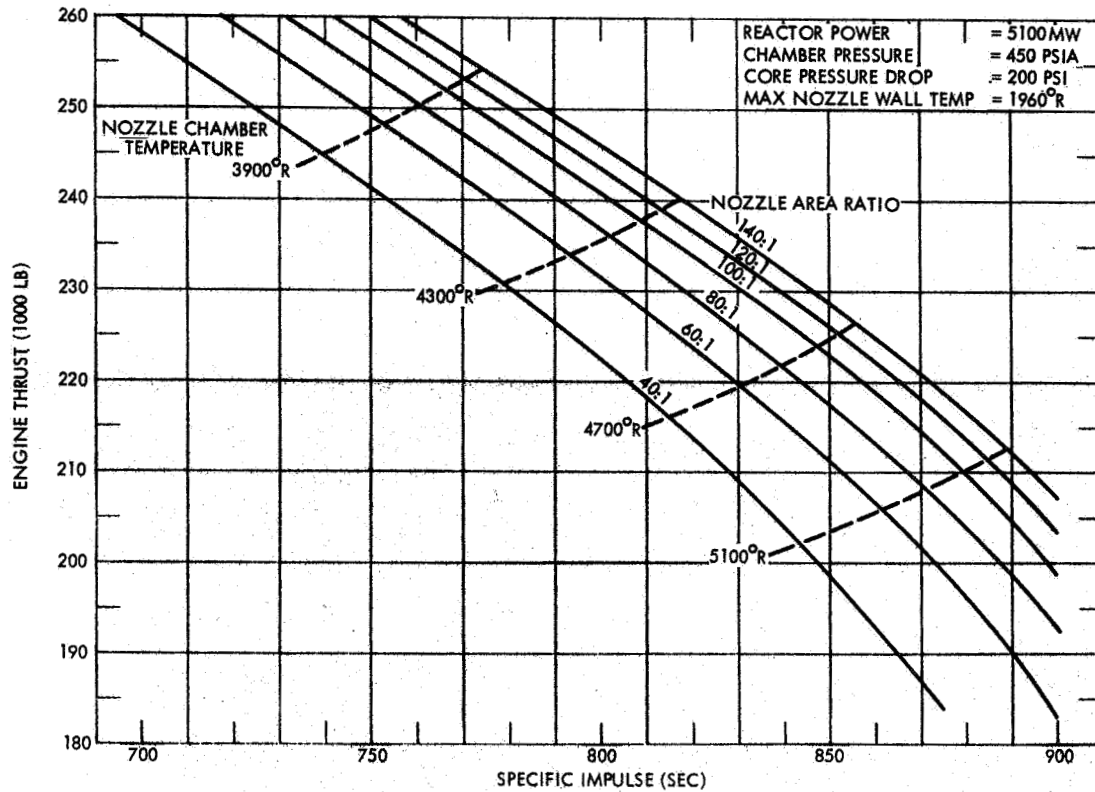
Figure V-11 Effect of Nozzle Expansion Ratio and
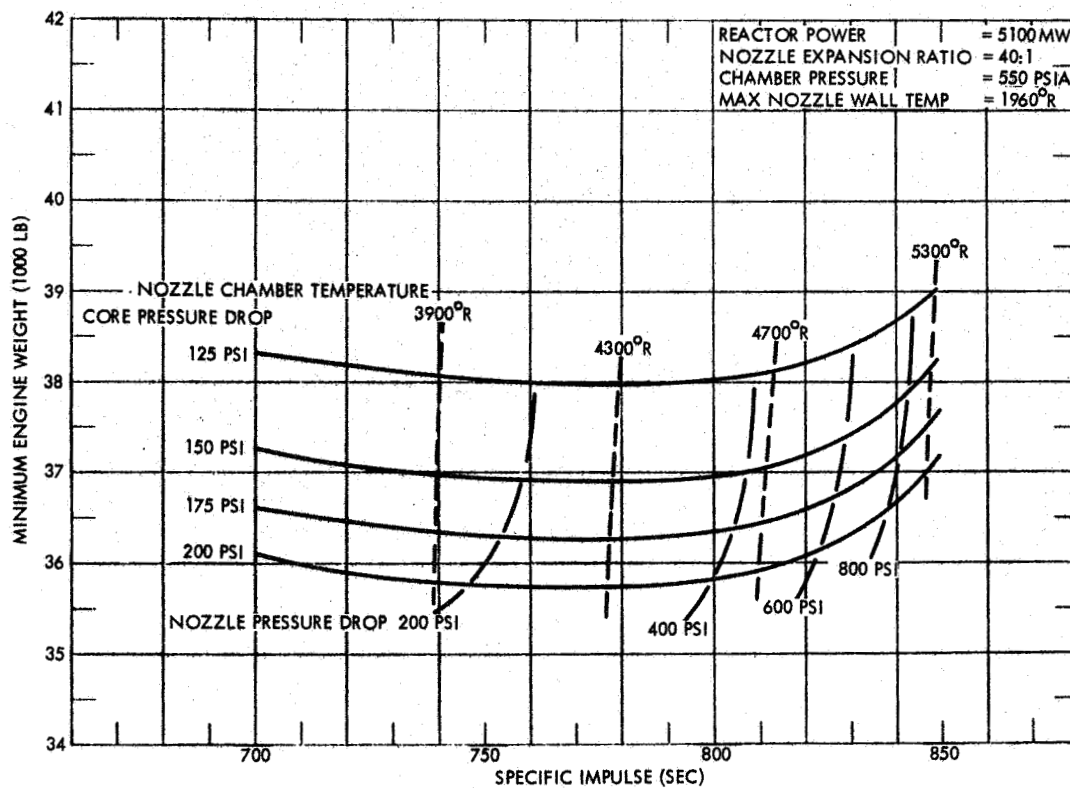Specific Impulse on Engine Thrust

Figure V-12 Effect of Core Pressure Drop and
Specific Impulse on Minimum Engine Weight

V-14

with increasing core pressure drop. Therefore, the core void fraction decreases and results in a reduction in the core dimensions and weight. These results indicate that significant weight savings can be realized by designing for higher core pressure drops. However, the reduction in engine weight with increasing core pressure drop is somewhat offset by the reduction in specific impulse for the same nozzle chamber temperature. The decrease in specific impulse results from the increased turbine bleed fraction required to deliver the higher pump discharge pressures necessary to provide the higher core pressure drop.

For the minimum weight engines, the variation of engine thrust with specific impulse and core pressure drop is displayed by Fig. V-13. The engine thrust and specific impulse are relatively insensitive to core pressure drop.
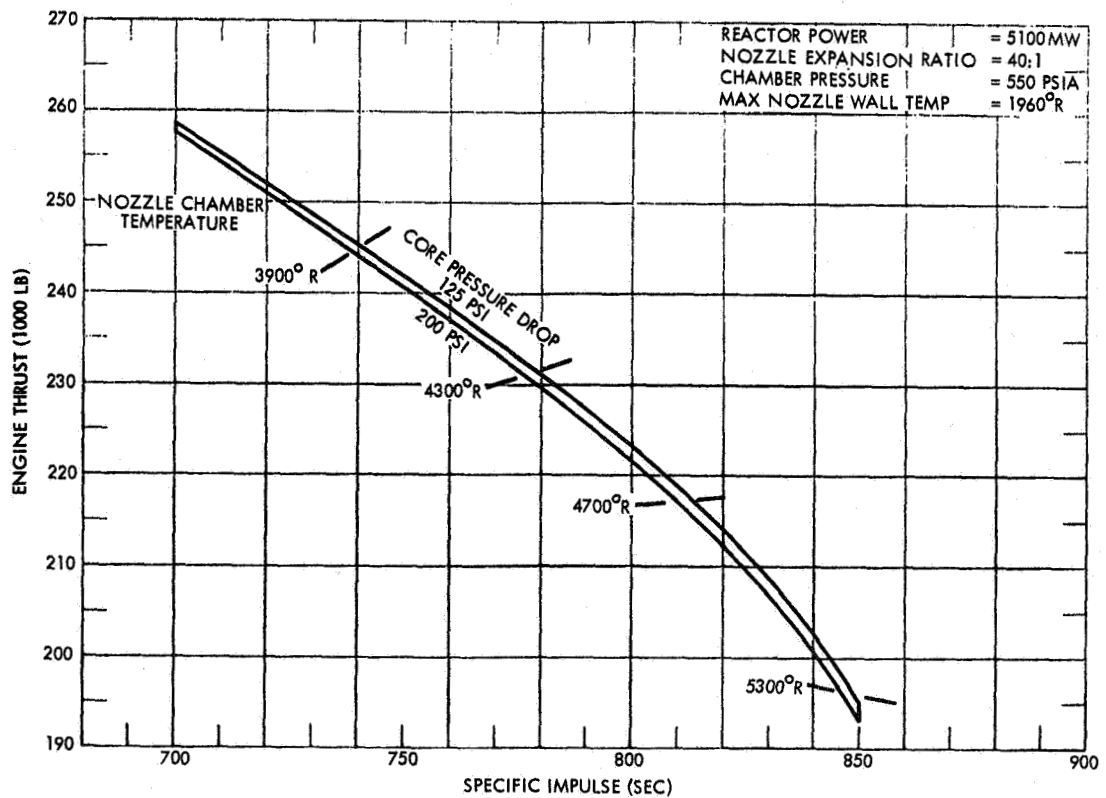

Figure V-13 Effect of Core Pressure Drop and Specific Impulse on Engine Thrust

The influence of the principal engine design parameters on engine weight and performance of a 5000 Mw class engine can be significant. Main nozzle expansion ratio was found to have the greatest effect on engine performance. For instance, an increase in nozzle expansion ratio produces higher specific impulse and thrust for the same chamber temperature; however, the engine weight is also increased.

Selection of the nozzle chamber pressure is extremely important because lighter weight engines delivering higher specific impulses can be realized for the same nozzle chamber temperature. The increase in specific impulse is, however, accompanied by a slight decrease in thrust. Increasing the core pressure drop decreases engine weight; however, the specific impulse attainable for a given chamber temperature is decreased.

To determine the optimum combination of engine parameters for specific design constraints, the effect of each engine parameter on engine weight and performance must be evaluated and then the resulting effect on the vehicle performance for a particular mission has to be determined.

INFLUENCE OF ENGINE PARAMETERS ON VEHICLE PERFORMANCE

The minimum weight vehicle is sensitive to the engine performance, i.e., the engine weight, specific impulse, and thrust. Using the engine weights, thrusts, and specific impulses associated with the minimum weight engines, the influence on initial vehicle weight in Earth orbit was determined as a function of the major engine variables. The influence of the engine parameters was investigated to determine their effect on a vehicle designed for a 1982 and 1986 manned Mars stopover mission. The results for only the 1982 mission are presented here; the results for 1986 mission were similar to those of 1982. The mission mode consisted of the following propulsive stages:

Depart Earth	-	Cluster of two nuclear engines
Arrive Mars	-	Single nuclear engine
Depart Mars	-	Single nuclear engine
Arrive Earth	-	Cryogenic retro braking to 15 km/sec plus aerodynamic braking

By determining the influence of the principal engine design parameters and constraints on vehicle performance, the combination of engine design variables which produced the highest performance nuclear engine consistent with the state-of-the-art was selected.

The effect of the variation in engine weight and performance on the initial vehicle weight in Earth orbit for the 1982 manned Mars mission is shown in Fig. V-14 as a function of chamber pressure. For a fixed chamber temperature, the higher specific impulses obtainable at the lower chamber pressures result in lower vehicle weights. For specific impulses less than 800 sec the effect of chamber pressure is relatively small. For higher values of specific impulse, the chamber pressure becomes increasingly important. For this class of engines, nozzle chamber pressures in the vicinity of 350 to 450 psia lead to minimum vehicle weight. For a nozzle chamber temperature of 4700° R, a reduction in nozzle chamber pressure from 700 to 450 psia resulted in an increase in specific impulse and a decrease in engine weight, producing a 110,000 lb reduction in vehicle weight. Due to the sensitivity of vehicle weight to specific impulse, the selection of the peak fuel element temperature constraint is extremely important because it determines the attainable exit gas temperature. Each 100° R increase in peak fuel temperature increases the specific impulse by 8 sec and results in vehicle weight savings of from 30,000 to 50,000 lbs.

The significant reduction in initial vehicle weight in Earth orbit obtained by increasing nozzle expansion ratio from 40:1 to 140:1 is shown by Fig. V-15 as a function of chamber temperature. It is possible to achieve an 8 percent vehicle weight saving by increasing the nozzle expansion ratio from 40:1 to 140:1. The results presented in this figure demonstrate that increasing the nozzle expansion ratio, for a fixed nozzle chamber temperature, has a diminishing effect on decreasing vehicle weight. At nozzle expansion ratios greater than 140:1 very little vehicle weight savings can be realized. It is also evident that the effect of nozzle expansion ratio becomes more significant at lower values of exit gas temperature.
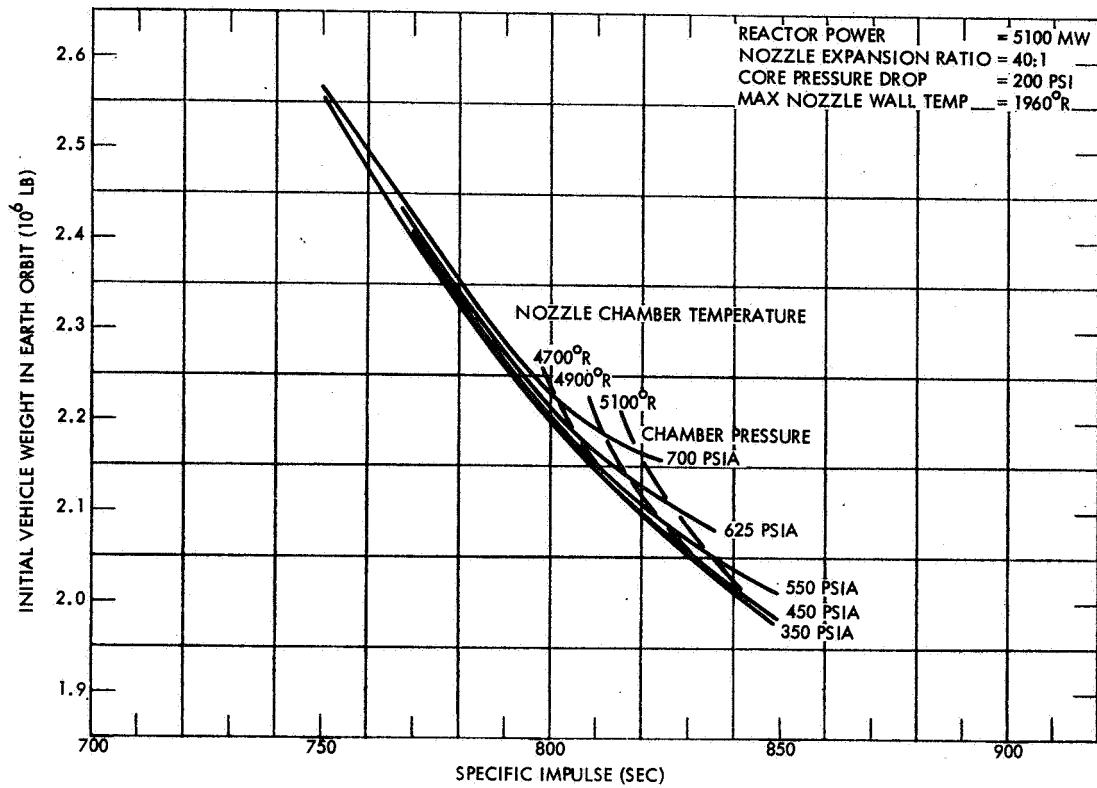
Figure V-14 Effect of Chamber Pressure and Specific
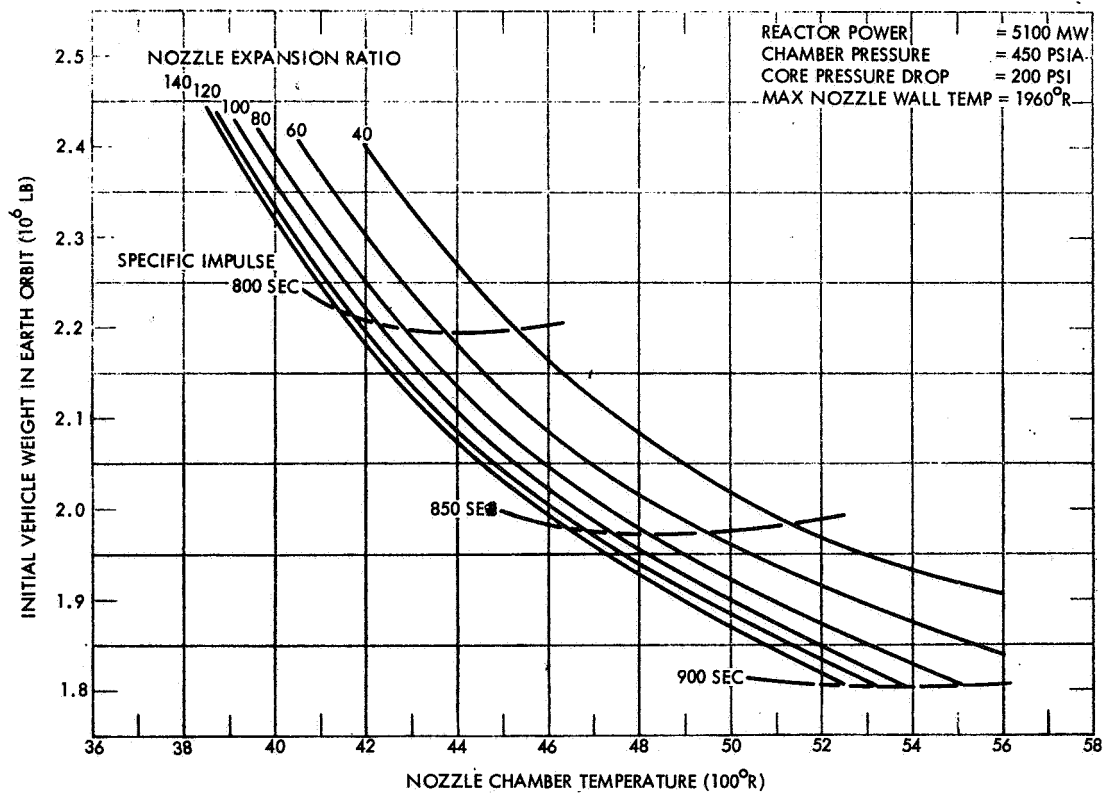Impulse on Initial Vehicle Weight in Earth Orbit

Figure V-15 Effect of Nozzle Expansion Ratio and Nozzle Chamber
Temperature on Initial Vehicle Weight in Earth Orbit

V-18

The sensitivity of initial vehicle weight in Earth orbit to core pressure drop is shown in Fig. V-16. Increasing the core pressure drop from 125 psi to 200 psi results in a vehicle weight decrease of 40,000 lb. The effect of core pressure drop is relatively insensitive to the specific impulse. For the range of core pressure drops investigated, higher pressure drops reduce the vehicle weight in Earth orbit.
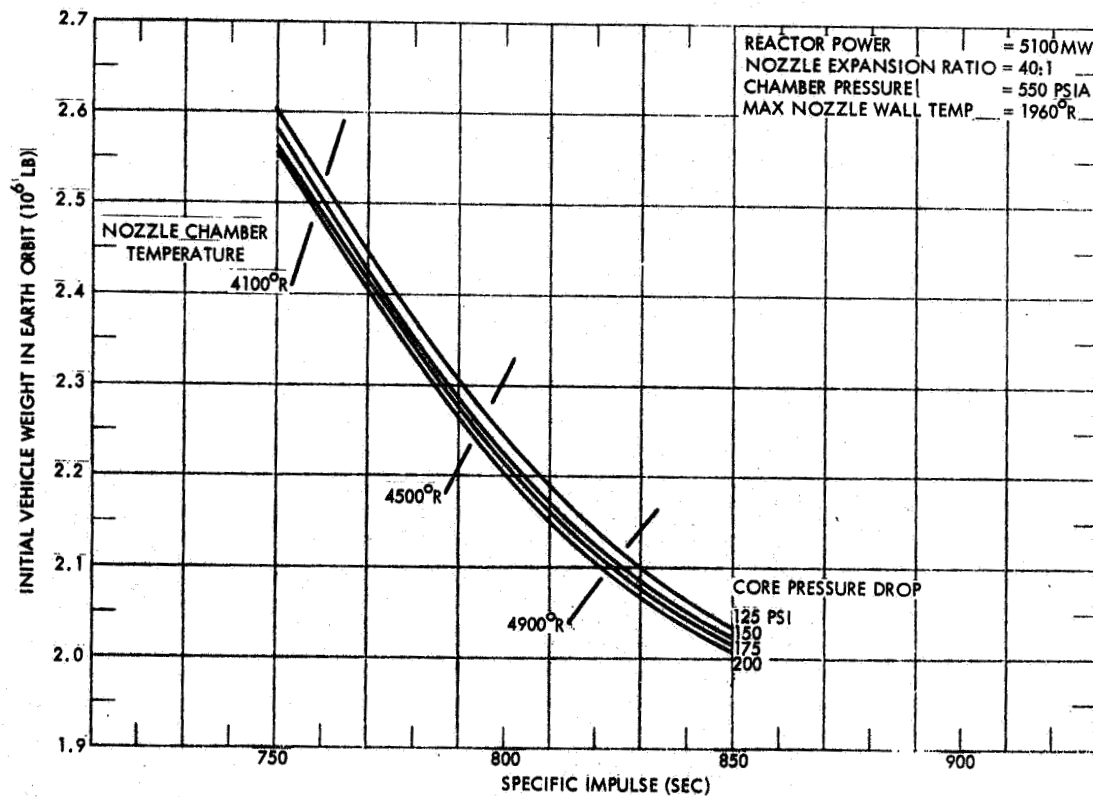
Figure V-16   Effect of Core Pressure Drop and Specific
Impulse on Initial Vehicle Weight in Earth Orbit

These results show that the engine parameters which significantly influence the specific impulse have the greatest effect on the initial vehicle weight in Earth orbit. The most influential engine design parameters which affect vehicle performance are the main nozzle expansion ratio and nozzle chamber pressure. Improper selection of these parameters can result in vehicle weight penalties as high as 5 to 10 percent of the total vehicle weight. Other engine parameters such as coolant channel diameter and core pressure drop primarily affect engine

weight, and thus, have a relatively small effect on vehicle weight. Typical variations in core pressure drop or coolant channel diameter produce changes amounting to 1 or 2 percent of the gross vehicle weight in Earth orbit.

The maximum available engine performance is a strong function of the engine state-of-the-art design constraints such as peak fuel temperature, fuel element web thickness, fuel element web temperature rise, and maximum allowable nozzle wall temperature. The design constraints which significantly influence specific impulse are extremely critical and require judicious selection. Selection of peak fuel temperature, fuel element internal and external web thickness, and the maximum allowable nozzle wall temperature are particularly crucial because their influence on vehicle performance is great. The fuel element web temperature rise primarily affects the engine weight and, therefore, has a smaller influence on the vehicle performance than the other design constraints.

A typical sensitivity of vehicle weight and engine performance to the major engine design parameters is shown in Table V-1 for the 1982 mission. These representative sensitivities, however, vary significantly with variations in mission, mission mode, mission year, and engine parameters.

ENGINE DESIGN CHARACTERISTICS

The selected engine was obtained using values of peak fuel temperature, nozzle wall temperature, fuel element web temperature rise, and fuel element web thickness determined from physical and manufacturing limitations which were considered to be representative of the future "state-of-the-art". The results of this study showed that the highest performance 5000 Mw engine is obtained using the maximum allowable values for peak fuel temperature, nozzle wall temperature, and fuel element web temperature rise; and using the minimum fuel element web thickness. Based on the selected design constraints, the engine characteristics which represent the best compromise thrust engine for the manned Mars stop-over mission are summarized in Table V-2.

Table V-1 Typical Engine Performance and Vehicle Weight Sensitivity*

Engine Parameter	Sensitivity			
	Specific Impulse	Engine Thrust	Engine Weight	Vehicle Weight
Peak Fuel Temp. (Exit Gas Temp)	$+0.08 \dfrac{\text{sec. } I_{sp}}{^\circ R}$	$-35 \dfrac{\text{lb. thrust}}{^\circ R}$	Negligible Effect	$-440 \dfrac{\text{lb. weight}}{^\circ R}$
Nozzle Expansion Ratio	$+0.40 \dfrac{\text{sec. } I_{sp}}{1}$	$+110 \dfrac{\text{lb. thrust}}{1}$	$+23 \dfrac{\text{lb. weight}}{1}$	$-1600 \dfrac{\text{lb. weight}}{1}$
Nozzle Chamber Pressure	$-0.06 \dfrac{\text{sec. } I_{sp}}{\text{psi}}$	$+10 \dfrac{\text{lb. thrust}}{\text{psi}}$	$+6.8 \dfrac{\text{lb. weight}}{\text{psi}}$	$+460 \dfrac{\text{lb. weight}}{\text{psi}}$
Core Pressure Drop	$-0.04 \dfrac{\text{sec. } I_{sp}}{\text{psi}}$	Negligible Effect	$-29 \dfrac{\text{lb. weight}}{\text{psi}}$	$-330 \dfrac{\text{lb. weight}}{\text{psi}}$
Maximum Nozzle Wall Temperature	$+0.01 \dfrac{\text{sec. } I_{sp}}{^\circ R}$	Negligible Effect	$-3 \dfrac{\text{lb. weight}}{^\circ R}$	$-100 \dfrac{\text{lb. weight}}{^\circ R}$

*1982 Mars stopover mission

Table V-2 Engine Characteristics

Engine Thrust	226,000 lb
Specific Impulse	850 sec
Engine Weight	37,500 lb
Nozzle Expansion Ratio	120:1
Reactor Power	5100 Mw
Nozzle Chamber Pressure	450 psia
Nozzle Chamber Temperature	4700° R
Core Pressure Drop	200 psi
Nozzle Wall Temperature	1960° R

REPRESENTATIVE VEHICLE DESIGN

A representative vehicle design using the selected engine for the 1982 manned Mars stopover mission was established. This vehicle utilizes the modular tank approach currently being investigated by NASA. It consists of the three main nuclear stages plus a payload stage which, continuing the modular concept, contains the midcourse stages, Mars lander, Earth reentry capsule, Earth retro braking stage, and mission module. The Earth retro stage decelerates the vehicle to 15 km per sec after which the payload module is landed aerodynamically.

Table V-3 lists the vehicle and stage weights for this representative vehicle and a drawing of the vehicle is in Fig. V-17.

Table V-3 Representative Vehicle Weight Statement

Stage	Description	Weight (lbs)
I	Leave Earth - Nuclear	973,308
II	Outbound Midcourse and Attitude Control-Storable	47,828
III	Arrive Mars - Nuclear	433,729
IV	Leave Mars - Nuclear	322,296
V**	Inbound Midcourse and Attitude Control-Storable	8,342
VI	Earth Retro - Cryogenic	30,804
Payload		206,749

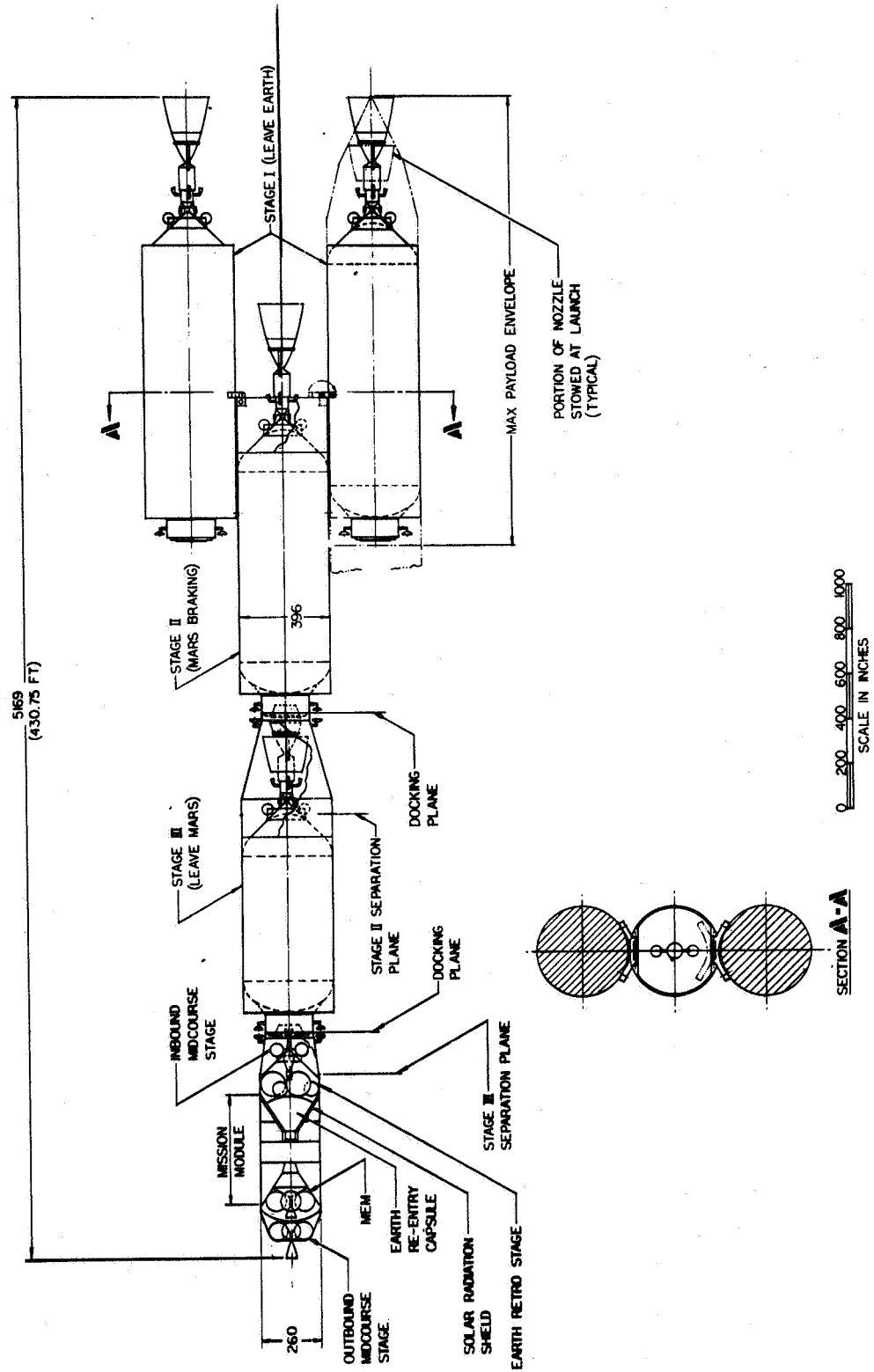|		
Mars Entry and Ascent Module	78,500	
Solar Radiation Shield	22,939	
Crew Compartment	68,734	
Life Support	22,750	
Reentry Capsule δ Earth Landed Payload	13,826	

INITIAL VEHICLE WEIGHT 2,023,056

Figure V-17 Representative Vehicle Design

VEHICLE SENSITIVITY

A comprehensive vehicle sensitivity analysis was performed. This analysis determined the effects on initial vehicle weight that are produced for variations in mission, vehicle, and performance parameters. The analysis was made for various mission years, vehicle configurations, and operational modes. The parameters that were varied included thrust, specific impulse, payloads, engine weight and clustering penalty, tank weight, stopover time, cryogenic storage thermal constants, and Mars aerodynamic capability.

As previously shown in Fig. V-1, the vehicle weight can increase by factors of two or three from a mission performed in the most favorable year (1986) to the least favorable (1978). Similar extreme variations in vehicle weight require-ments can also result for any given year for the extreme possibilities of Earth aerodynamic braking capabilities.

The effect on initial vehicle weight of changes in specific impulse, engine thrust, engine weight, Mars entry module weight, mission module weight, and Earth recovered weight is shown in Fig. V-18 for the Mars opposition year of 1982. An all nuclear vehicle is assumed with an aerodynamic braking capability at Earth of 15 km per sec.

Figure V-18 shows that of the three engine performance parameters, specific impulse, thrust, and engine weight, changes in the specific impulse produces the largest effect on vehicle weight. Typically, a 2 percent (15 sec) increase in specific impulse decreases the initial vehicle weight by 3.5 percent. In order to decrease the vehicle weight by this same amount the thrust would have to be increased by 6.5 percent (150,000 lb) or the engine weight reduced by 12 percent (4000 lbs).

The trade-offs between the engine performance parameters and payload weights as they vary from their nominal values is shown in this figure. For example, an increase of 2500 pounds in Earth-landed payload increases the initial vehicle weight by 3.5 percent. Therefore, either specific impulse or the thrust would have to be increased or the engine weight decreased by the amounts stated above to offset this increase. Alternatively, the vehicle weight increase can be offset by reducing the Mars entry module by 20,000 pounds.

NOMINAL INITIAL VEHICLE WEIGHT - 2.026 x 10⁶ LB

MARS STOPOVER MISSION 1982

DEPART EARTH	- NUCLEAR (2 ENGINES)
ARRIVE MARS	- NUCLEAR
DEPART MARS	- NUCLEAR
ARRIVE EARTH	- AERO PLUS CHEMICAL RETRO TO 15 KM/SEC

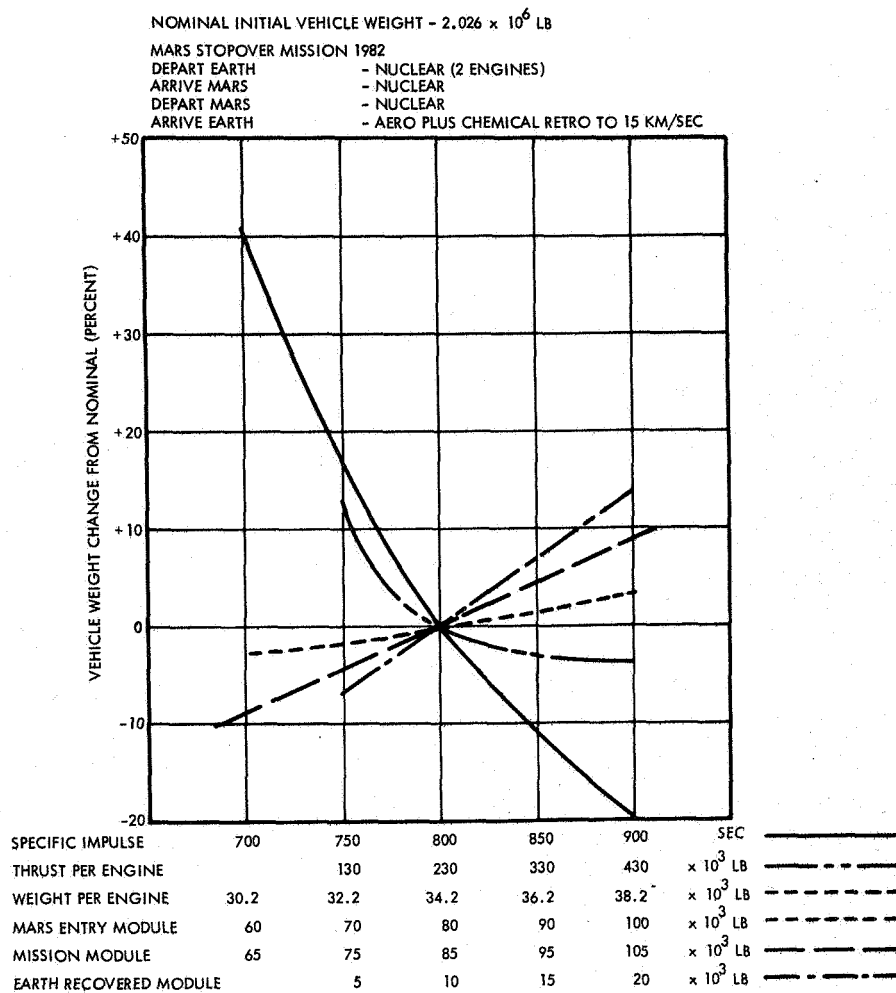|						
SPECIFIC IMPULSE	700	750	800	850	900	SEC
THRUST PER ENGINE		130	230	330	430	x 10³ LB
WEIGHT PER ENGINE	30.2	32.2	34.2	36.2	38.2	x 10³ LB
MARS ENTRY MODULE	60	70	80	90	100	x 10³ LB
MISSION MODULE	65	75	85	95	105	x 10³ LB
EARTH RECOVERED MODULE		5	10	15	20	x 10³ LB

Figure V-18 1982 Vehicle Weight Sensitivity

The use of aerodynamic braking at Mars can result in comparatively large vehicle weight reductions. Use of this braking mode reduces the vehicle weight for the cryogenic propellant vehicle by 50 percent in 1986 and by over 66 percent in 1978. In contrast, the nuclear vehicle weight is reduced by 20 percent in 1986 and by 50 percent in 1978. These results are based on a K = 1 in the aerodynamic braking scaling law. If a more "efficient" braking system could be developed, further weight savings would result.

Figure V-19 shows the effect on vehicle weight for variations in the tank jettison weight as functions of mission year. Approximately 20 percent more vehicle weight is required for the 1986 mission for a vehicle whose propellant tank mass fractions are decreased by about 10 percent (mass fraction case no. 1 to case no. 3). This same decrease in propellant tank mass fractions increases the vehicle weight by over 150 percent for the most unfavoraale mission year, 1978.
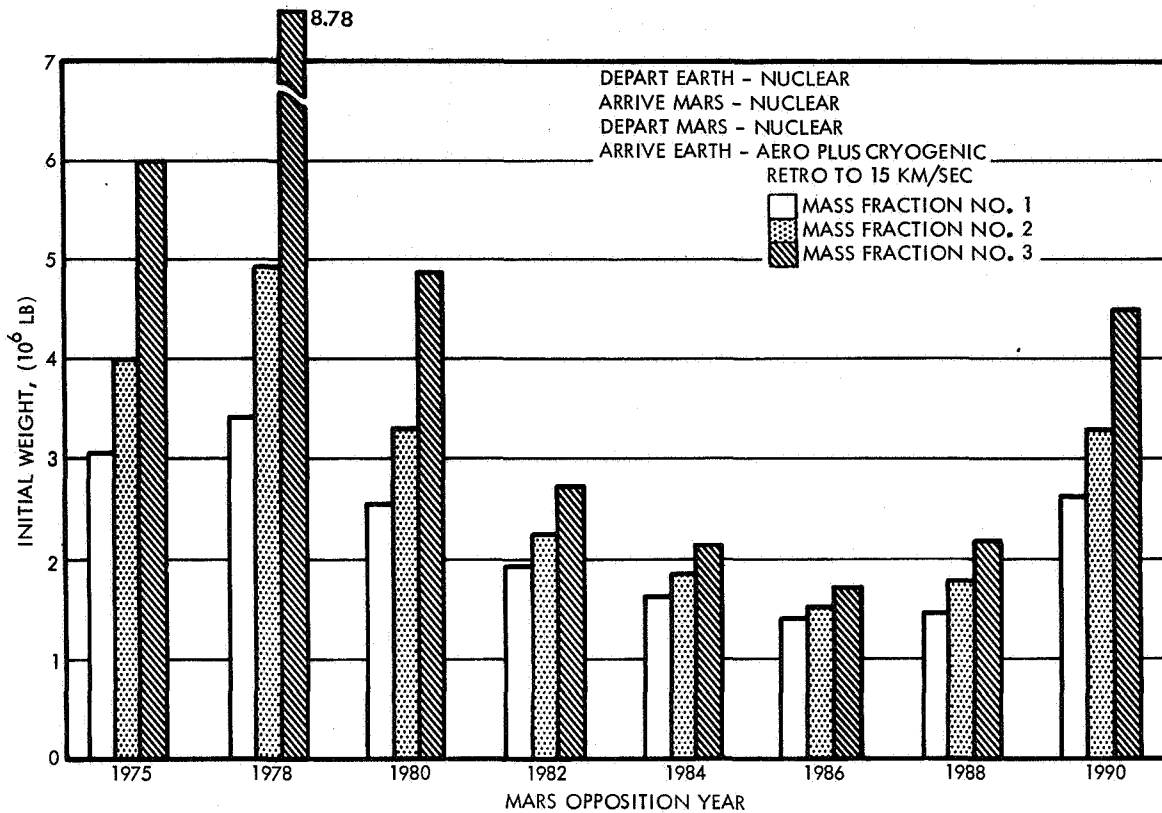
V-25

Figure V-19 Vehicle Weight vs Mass Fraction and Mission Year

Figure V-20 shows the effect on vehicle weight of variations in the tank jettison weight as a function of several combinations of vehicle propulsive and Mars aerodynamic braking modes.

These results show that the vehicle weight can be significantly increased due to discrete system weight increases. Particularly important are the weight provisions required for micrometeoroid protection and cryogenic propellant storage. Both the operational environment and the required technology concerning these two areas are currently not available. Therefore, the weight estimates assumed for these systems in this and other studies could be considerably in error.

A 20 percent increase in the arrive and depart Mars hydrogen tank weights due to increased micrometeoroid protection requirements would increase the initial vehicle weight requirements by 5.5 and 10.5 percent for the years 1986 and 1978, respectively.
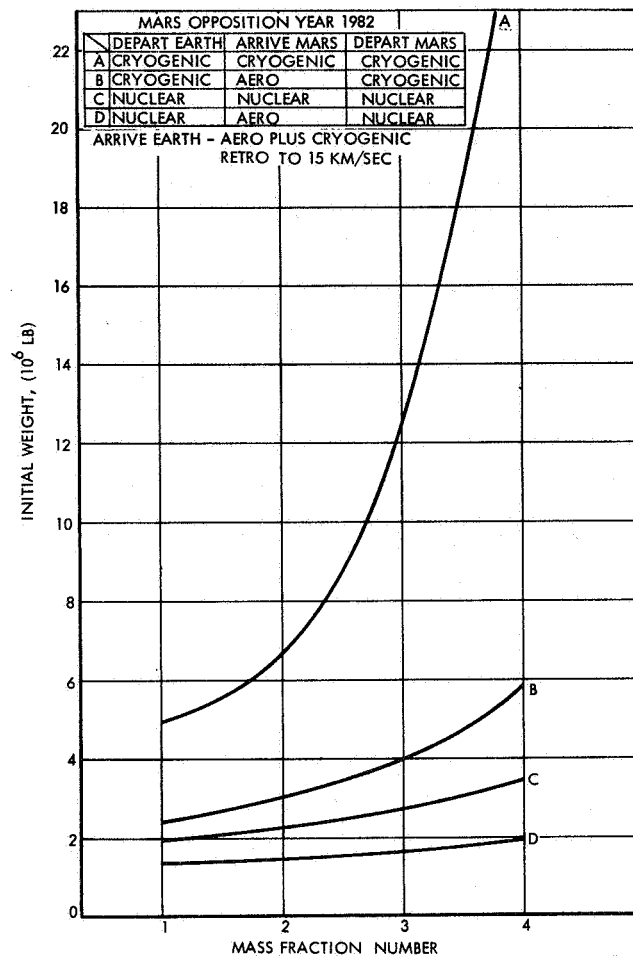
V-26

MARS OPPOSITION YEAR 1982		
	DEPART EARTH	ARRIVE MARS	DEPART MARS
A	CRYOGENIC	CRYOGENIC	CRYOGENIC
B	CRYOGENIC	AERO	CRYOGENIC
C	NUCLEAR	NUCLEAR	NUCLEAR
D	NUCLEAR	AERO	NUCLEAR

ARRIVE EARTH – AERO PLUS CRYOGENIC RETRO TO 15 KM/SEC

Figure V-20 Vehicle Weight vs Mass Fraction and Vehicle Mode

VENUS SWINGBY MISSIONS

An incomplete analysis indicated that some of the extremes in vehicle weight variations due to the unfavorable years or high Earth arrival velocities could be eliminated and the overall vehicle weight requirements reduced by resorting to the Venus swingby trajectories. Reductions in vehicle weight of over 20 percent were found to be possible for some of the cases investigated. The investigations made during the study were by no means exhaustive and future effort in this area is certainly desirable in order to determine the ultimate potential of the Venus swingby mode.

COMPUTER PROGRAMS

The mission and engine optimization and analysis techniques and computer programs (NOP, FLOP, and SWOP) which were developed during this study provide a significant major advancement over previously available methods for performing vehicle and engine systems analysis. These techniques allowed a comprehensive investigation of the influence of the engine and vehicle characteristics on the vehicle performance for a wide range of missions. During the study, the programs were modified several times to broaden their scope by including additional engine types and flow schemes, a greater number of mission types and vehicle configuration options, and additional independent parameters in the mission optimization process. The programs as they now exist, as well as with further anticipated modifications, will serve as valuable tools for future analysis and investigation of interplanetary missions, space vehicle designs, and solid core nuclear engine designs.

PARAMETRIC DATA BOOKS

Finally, an important product developed during the course of the study is the compilation of all of the mission, vehicle, and engine parametric data which were generated into two selfconsistent data books, Vols III and V of this series of final reports.

REFERENCES

1. Module Designs for Assembly into Nuclear Orbital Vehicle, Lockheed Missiles and Space Company, LMSC/A650541, 11 June 1964, NAS8-9500.

2. Space Flight Handbooks, Planetary Flight Handbook, Vol. 3, NASA SP-35, prepared for George C. Marshall Space Flight Center, Huntsville, Alabama under Contract NAS8-5031.

3. Frank W. Gobetz, Optimum Transfers Between Hyperbolic Asymptotes, AIAA Journal, Vol. 1, September 1963, p. 2034.